TECHNICAL REPORT ECOM- 8 - 0547

EQUIPMENT COMPLIANCE REPORT

AZIMUTH AND ELEVATION DIRECTION FINDER TECHNIQUES

(Developmental Model)

By

J. E. Ferris, W. B. Henry and W. E. Zimmerman

January, 1969

ECOM

UNITED STATES ARMY ELECTRONICS COMMAND FORT MONMOUTH , N.J.

CONTRACT DA AB07-67-C0547 DA Project 5A6 79191 D902-05-11

THE UNIVERSITY OF MICHIGAN
DEPARTMENT OF ELECTRICAL ENGINEERING
RADIATION LABORATORY
ANN ARBOR, MICHIGAN

EQUIPMENT COMPLICANCE REPORT

SUMMARY

This report describes the testing procedures and test results employed to evaluate the performance of an Azimuth-Elevation Direction Finding (A-EDF) system developed by The University of Michigan Radiation Laboratory. The A-EDG system consists of an antenna system, electromechanical switch, video amplifier, A/D converter, computer and azimuth-elevation display system. The A-EDF system is designed for use in the detection, frequency measurements, and determination of bearing (azimuth and elevation) of radio frequency (RF) transmissions from fixed, mobile or portable airborne sets operating in the frequency range of 0.6 to 3.0 GHz.

Since successful system operation depends on the performance of the sub-systems, the design goals include specifications for the subsystems as well as the total system performance. It is to be emphasized that the series of tests conducted were not designed to provide an exhaustive description of the A-EDF equipment, but rather were conceived as design aids during the development of the exploratory model. The report discusses the testing procedures utilized to evaluate and determine the degree of compliance of the antenna array, the data processing system, and the overall performance of the A-EDF system.

Two types of tests were performed for the evaluation of the A-EDF system; 1) free space tests and 2) fly-by tests. The purpose of the free space tests was to determine system accuracy and an ideal environment. The results of the free space tests suggest that the system has an accuracy of $\pm 5^{o}$ in both azimuth and elevation. The fly-by tests were performed to determine the effect of reflections on the A-EDG system performance under dynamic environmental conditions. However, it is difficult to assess the contribution of the ground reflection alone due to the electrically hostile environment in which the A-EDG system was operated.

TABLE OF CONTENTS

AZIMUTH AND ELEVATION DIRECTION FINDER TECHNIQUES

EQUIPMENT COMPLIANCE REPORT

1.0 INTRODUCTION

This report describes the testing procedures and test results employed to evaluate the performance of the A-EDF system developed at The University of Michigan in terms of the design goals set forth in Contract DAAB07-67-C-0547 "Azimuth and Elevation Direction Finder Techniques". Since the task described in the contract is for the development of an exploratory developmental model, there has been no officially approved test plan. It is to be emphasized that the following series of tests were not designed to provide an exhaustive description of the A-EDG system performance, but rather were conceived as design aids during the development of the exploratory model.

The A-EDF system is comprized of two main subsystems; one for data acquisition, which is the antenna array, and the other for data processing including a receiver (GFE), memory voltmeter, analog-to-digital converter, and computer. Since successful system operation depends on the performance of the subsystems, the design goals include specifications for the subsystems as well as total system performance. The following chapters of this report discuss, in order, the testing procedures utilized to evaluate and determine the degree of compliance of the antenna array, the data processing subsystems, and the overall performance of the A-EDF system. At the end of the report we present our conclusions and recommendations drawn from these tests.

2.0 DATA ACQUISITION SUBSYSTEM

This chapter describes contract design goals for the data acquisition subsystem, the tests used to evaluate the subsystem, and the degree to which this subsystem complies with those design goals.

2.1 Antenna Array Elements

The contract design goals for the antenna array elements include a VSWR of no greater than 3:1, an axial ratio of 3 dB for the circularly polarized elements, and a gain of not less than 5 dB above a circularly polarized isotropic source. All of these specifications apply across the entire 5:1 operating bandwidth of 600 to 3000 MHz.

The VSWR of the elements was measured with a slotted line employing the equipment arrangement shown in Fig. 2-1. Care was taken to insure the antenna was in an essentially free space environment. The measurements were repeated only for a few of the 17 elements because of the excellent agreement from element to element. Typical VSWR data is shown in Fig. 2-2 for 100 MHz increments across the 5:1 band. The maximum VSWR is 2.80 and occurred at 2800 MHz.

The axial ratio of the antenna was measured by rotating the antenna about an axis normal to the plane of the element spiral in 10^{o} increments and rotating the spiral continuously in the plane containing the axis. This allowed the axial ratio to be measured not only at the peak of the beam, but at all other points as well. The maximum axial ratio measured at the peak of the beam of the sample of elements measured is tabulated versus frequency in Table 2.1 for the discrete frequencies of 0.6, 1.6, 1.8 and 3.0 GHz. The maximum axial ratio is 1 dB for the frequencies measured.

TABLE 2.1: SPIRAL AXIAL RATIO VS FREQUENCY

Frequency (GHz)	0.6	1.6	1.8	3.0
Axial Ratio (dB)	0.5	1.0	0.5	1.0

The gain of the elements was measured by the substitution method. A pattern of an antenna with a known gain (in this case a gain standard horn) was superimposed on a pattern of the element antenna. The directive gain at the peak of the beam is then the difference in received signal levels at that point. The equipment arrangement is given in Fig. 2-3. The gain of the elements measured is 3 dB above a linearly polarized isotrope at 1.1 and 1.6 GHz. Since the gain of a linearly polarized isotrope is 3 dB above a circularly polarized isotrope, the gain of the elements is 6 dB above a circularly polarized isotrope source at these frequencies.

Another important parameter of the element antennas employed in this direction finder system is squint. Pattern measurements for one antenna orientation were repeated at 100 and 200 MHz increments across the 5:1 frequency band specified. The results appear in Fig. 2-4.

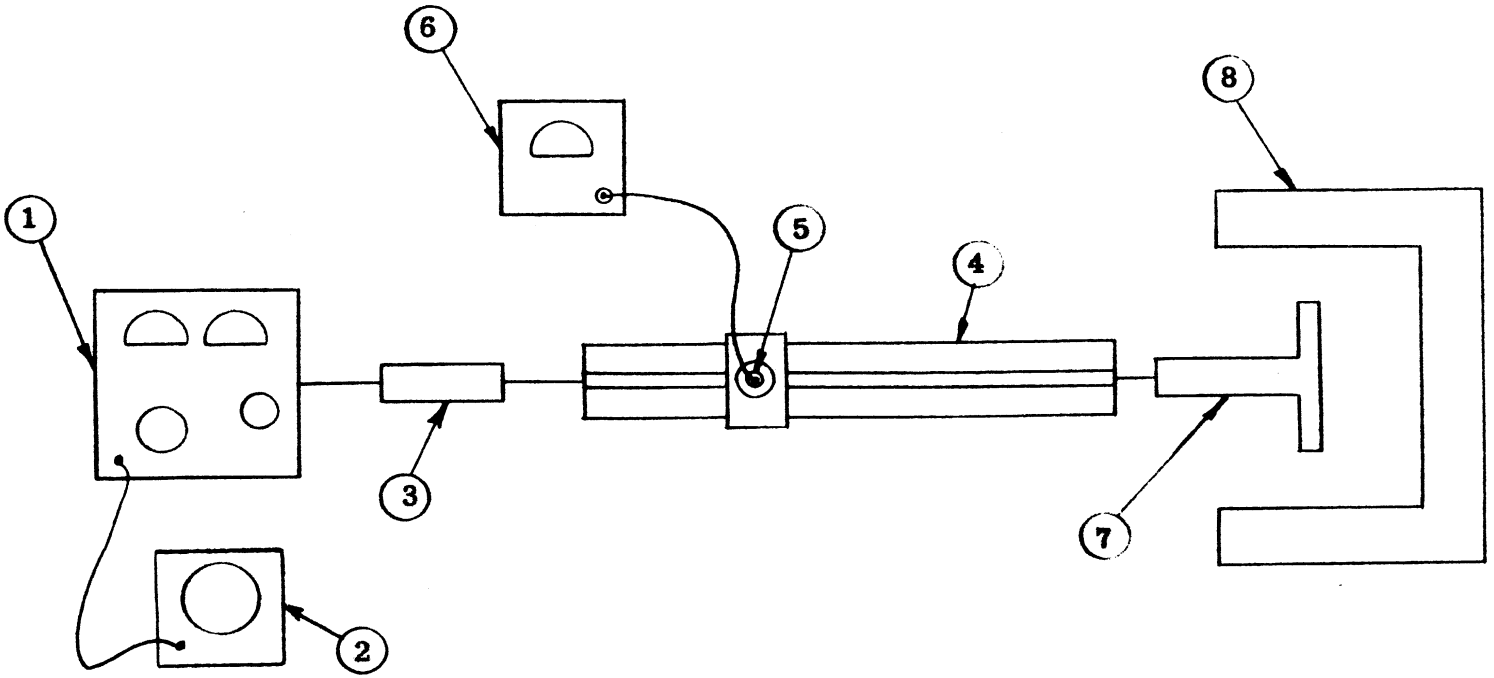

FIG. 2-1: VSWR Test Set (continued on next page).

VSWR TEST SET

Legend	Equipment Description	Frequency Range	Manufacturer	Model	Serial
1 a	VHF Signal Generator	10 - 480 MHz	Hewlett-Packard	608A	1577
1 b	UHF Signal Generator	450 - 1230 MHz	Hewlett-Packard	612A	299-01770
1 c	UHF Signal Generator	800 - 2100 MHz	Hewlett-Packard	614A	289-02172
1 d	UHF Signal Generator	1.8 - 4.1 GHz	Hewlett-Packard	616B	007-00893
2	Wide Range Oscillator	5 - 60,000 Hz	Hewlett-Packard	200CV	229-41280
3	3dB Attenuator	DC - 3.0 KMc	Weinschel	50-3	D2567
4	Slotted Line	500 - 4000 MHz	Hewlett-Packard	805A	226
5 a	Bolometer	50 - 1000 MHz	Hewlett-Packard	476A	
5 b	Bolometer	.5 - 10 GHz	PRD	627A	2775
6	Standing Wave Indicator	1000 Hz	Hewlett-Packard	415B	483
7	Test Antenna	600 - 3000 MHz			
8	Shielded Anechoic Enclosure	500 - 12000 MHz			

FIG. 2-1 (continued) Description of VSWR Test Set.

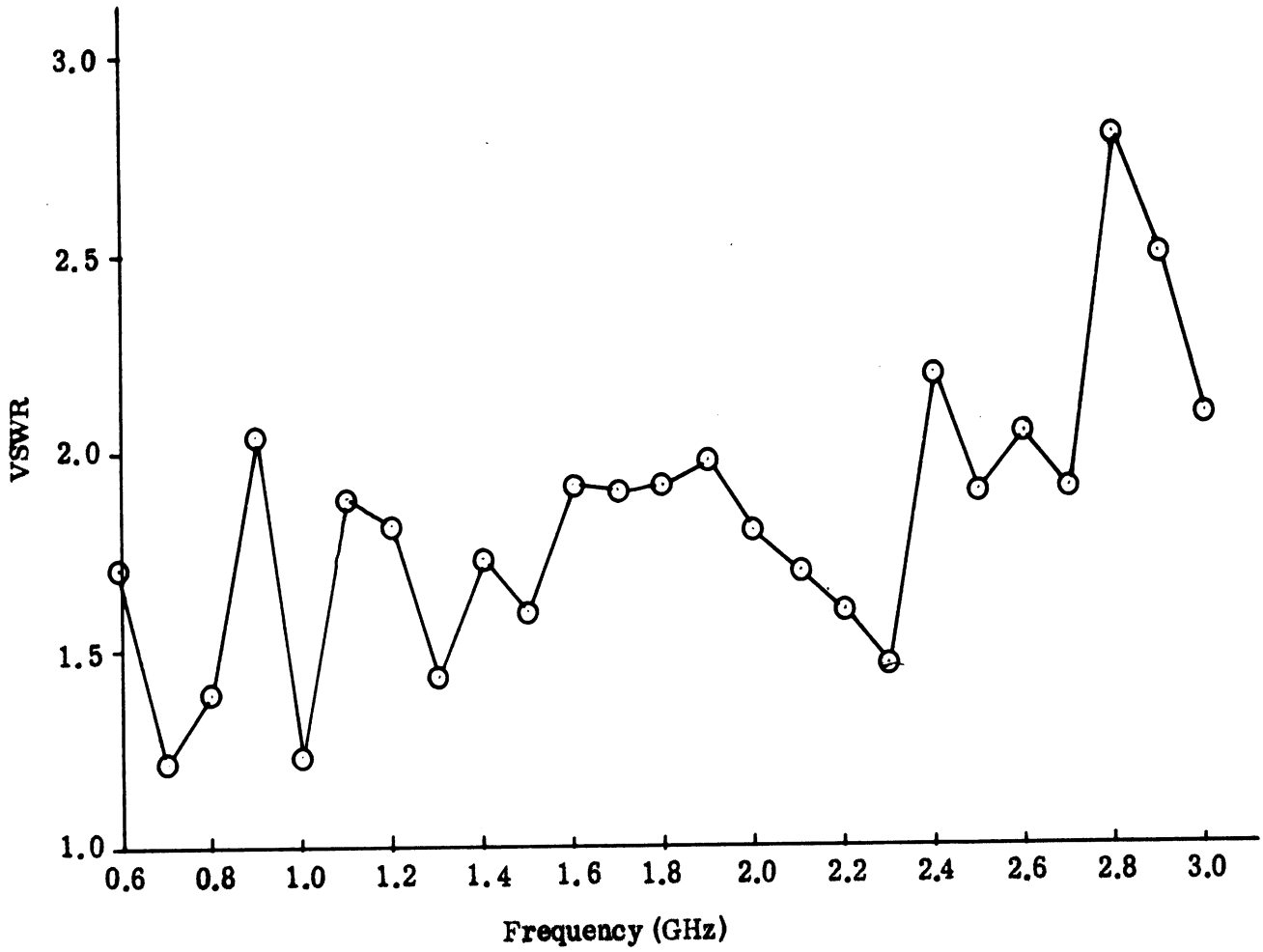

FIG. 2-2: Spiral VSWR versus Frequency.

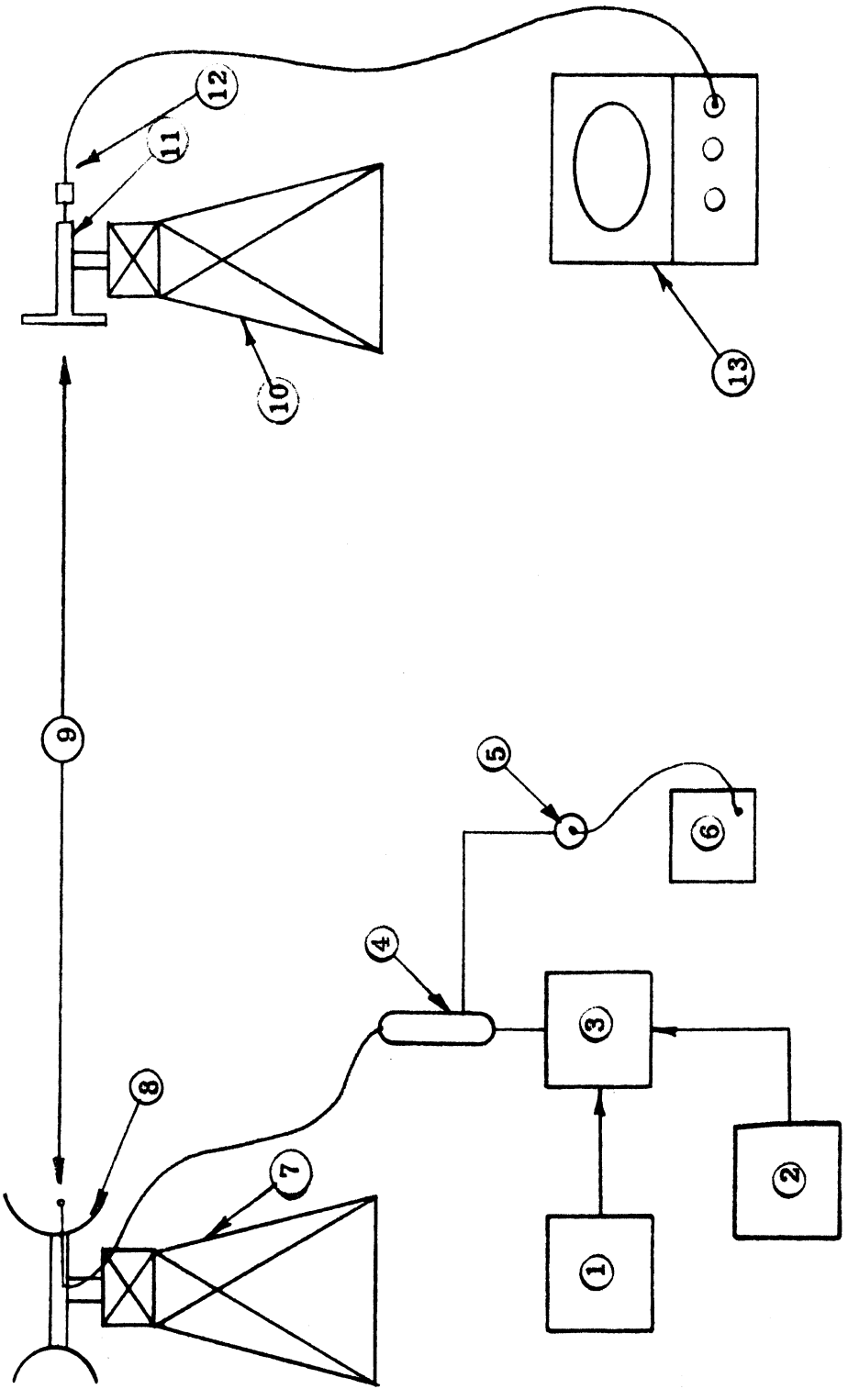

FIG. 2-3: Pattern and Gain Measurement Test Set
(continued on next page).

GAIN AND PATTERN MEASUREMENT TEST SET

Legend	Equipment Description	Frequency Range	Manufacturer	Model	Serial
1	Regulated Power Supply		G.R.	1201B	1451
2	Fork Modulator	1000 Hz	Antlab	2707	158
3 a	Unit Oscillator	250 - 920 MHz	G.R.	1209B	
3 b	Unit Oscillator	900 - 2000 MHz	G.R.	1218A	
3 c	Microwave Oscillator	1.7 - 4.1 GHz	G.R.	1360B	486
4	Directional Coupler	1.0 - 4.0 GHz	Narda	3022	110
5	Bolometer	50 - 1000 MHz	H.P.	476A	
6	Standing Wave Indicator		H.P.	415B	483
7	40' Transmitting Tower				
8 a	15' Parabolic Dish	500 - 1500 MHz			
8 b	10' Parabolic Dish	1500 - 2500 MHz			
9	200' Transmitting Dist.				
10	40' Receiving Tower				
11 a	Test Antenna				
11 b	L band Gain Standard Horn	1.12 - 1.70 GHz	Built to NRL Spec.		
12	Bolometer	.5 - 10 GHz	PRD	627A	2775
13	Antenna Pattern Recorder		Antlab	2375A	301

FIG. 2-3 (continued) Description of Pattern and Gain Measurement Test Set.

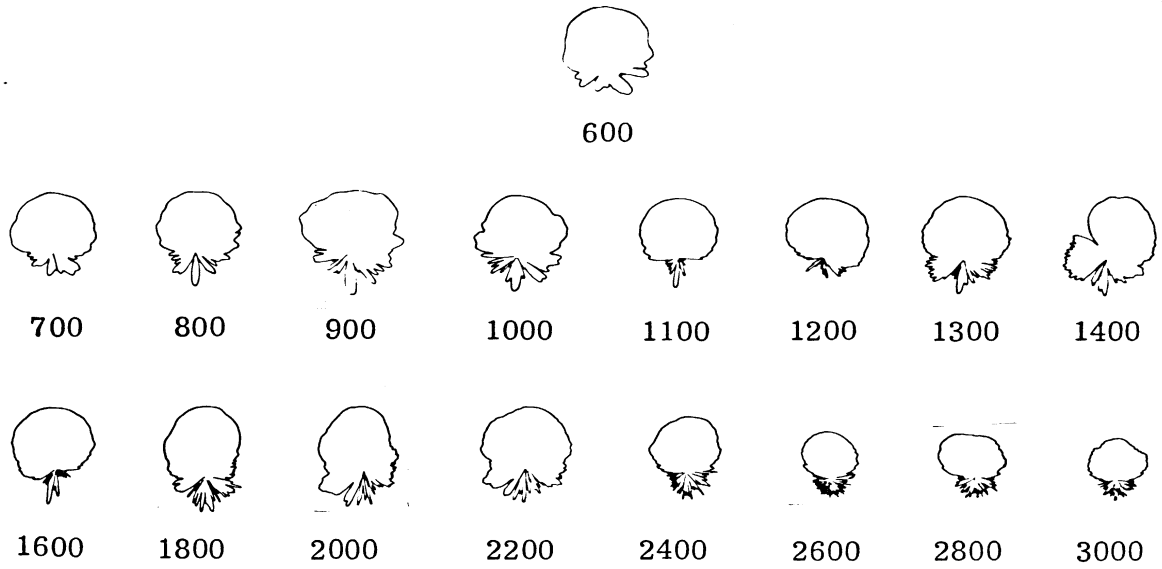

FIG. 2-5: 15 Turn Cavity Backed Spiral with a Duncan - Minerva Balun Mounted at the Zenith of a 6 Foot Hemisphere (E-Plane Patterns for a 5:1 Frequency Band).

2.2 Hemispherical Array

The contract design goals covering the array suggests that the array shall consist of a minimum of 16 broadband, cavity-backed, flat spiral antenna elements, mounted on a 6' diameter hemispherical ground plane. The actual array delivered consists of 17 broadband, cavity-backed, flat spiral antenna elements mounted on a 6' diameter hemispherical ground plane. A photograph of the completed array is shown in Fig. 2-5.

Also specified is that the array shall be capable of being scanned electronically. Because of the cost and complexity of developing a broadband purely electronic (e. g. diode) switching arrangement, a electromechanical unit has been substituted. This unit provides reliable operation over the entire 5:1 operating band, displays low insertion loss and has provisions for varying the scanning rate. The scanning rate should be fast enough to prevent amplitude modulation due to a scanned source, but slow enough to accommodate all manner of signal modulation. The scanning rate has been optimized at 1000 scans per second, with provisions for varying this rate at the discretion of the operator.

3.0 DATA PROCESSING SUBSYSTEM

This chapter describes the contract design goals for the data processing subsystem and the degree to which this subsystem complies with those specifications.

The contract design goals include a system which shall obtain the relative amplitude information from the elements of the antenna array. This information shall be processed and presented in a form to the visual bearing indicator unit suitable to permit the visual presentation of the azimuth and elevation direction of arrival of the received signals. Additionally, the information fed to the visual bearing indicator unit shall be read out in numerical form. The data processing subsystem is shown in block diagram in Fig. 3-1. The relative amplitude information is received, amplified, measured and processed. The azimuth and elevation information is presented in visual numerical form by a NIXIE tube presentation on the front of the cabinet. The information can also be automatically printed out on the system teletype at the discretion of the operator. A CRT visual bearing indicator was rejected as providing only redundant information at a low precision and high cost.

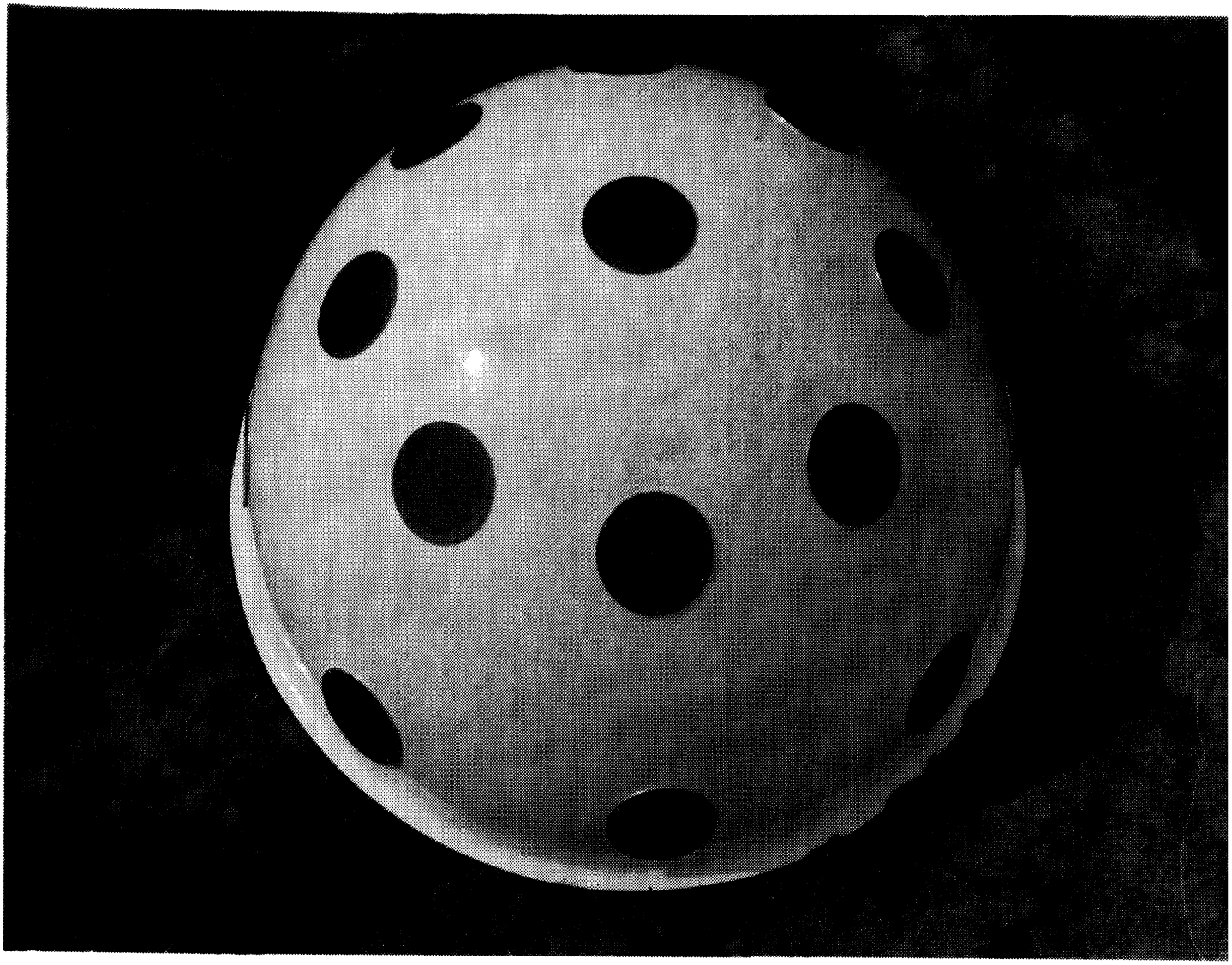

FIG. 2-5: Complete Hemispherical Array.

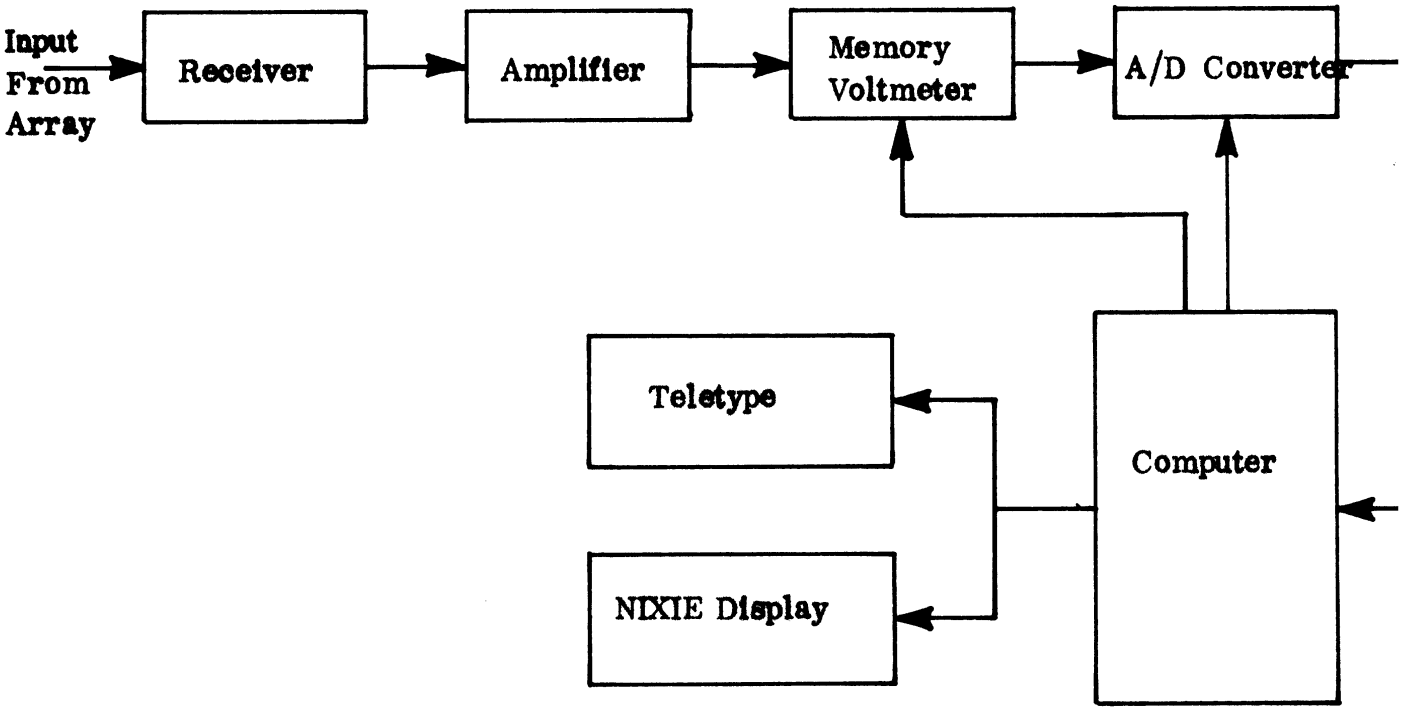

FIG. 3-1: Block Diagram of Data Processing Subsystem.

4.0 PERFORMANCE OF THE A-EDF SYSTEM

This chapter describes the contract design goals for the entire A-EDF system, the tests used to evaluate system performances, and the degree to which this subsystem complies with the specifications.

The design goals for the A-EDF system include a $\pm 2^{o}$ bearing accuracy in azimuth over 360^{o} of azimuth coverage and $\pm 5^{o}$ bearing accuracy in elevation for 90^{o} of elevation coverage. It is desirable to hold these tolerances over a frequency range of 600 - 3000 MHz for signals containing pulse, CW, AM and FM modulation waveforms. Also, environmental requirements are supplied in the contract (i.e. temperature, wind load, etc) but no effort was expended to determine if this exploratory developmental model conformed to those specifications.

4.1 Free-Space Performance

The first series of tests with the A-EDF system were made under simulated free space conditions by installing the array on the general purpose antenna range shown in Figs. 4-1 and 4-2. The electromechanical switch used for scanning the array is located on the tower near the array in Fig. 4-1. The data processing equipment is housed in the building at the lower left of the photo.

With a CW signal source operating at 1.6 GHz, the array was scanned in elevation at a constant azimuth. The coordinate system used to describe this data is shown in Fig. 4-3. Figures 4-4 through 4-7 are plots of the variations in recorded azimuth as a function of the true elevation angle. For example, referring to Fig. 4-4, the scan starts at an elevation of 90^{o} and an azimuth of 90^{o}, corresponding to the circle in the lower right hand side of the graph. As the scan progresses, the elevation decreases in the direction of the arrows until the elevation passes through zero and the azimuth jumps to 270^{o}. The scan is completed as the elevation continues to decrease from zero to 90^{o}. Ideally the azimuth data should read either 90^{o} or 270^{o}, depending on the side of the hemisphere (east or west) data is being collected from. The data near the pole position of the hemisphere (i.e. data looking straight above the hemisphere, $\theta=0^{o}$) is least accurate. Additional data collected at 1.6 GHz for azimuth angles of 80^{o}, 70^{o} and 60^{o} is shown in Figs. 4-5 through 4-7.

Figures 4-8 through 4-11 are graphs of the calculated elevation angles as a function of the true elevation for azimuth angles of 90^{o}, 80^{o}, 70^{o} and 60^{o}. The cause for the deviation of the calculated elevation angles from the true elevation is the non-symmetrical location of antennas in the θ plane of the antenna system. That is, the antenna elements are only employed in the upper hemisphere of the spherical coordinate system. These deviations are predictable and the necessary corrections have since been programmed into the computer. For purposes of comparison, the theoretically computed elevation angle versus the actual elevation angle, assuming a cosine antenna pattern for the individual elements is included in Fig. 4-12. Note that the measured elevation does indeed conform well to the theoretical data of Fig. 4-12.

FIG. 4-1: Photograph of Antenna Range used for A-EDF System Free Space Measurements.

FIG. 4-2: Photograph of Antenna Range used for A-EDF System Free Space Measurements.

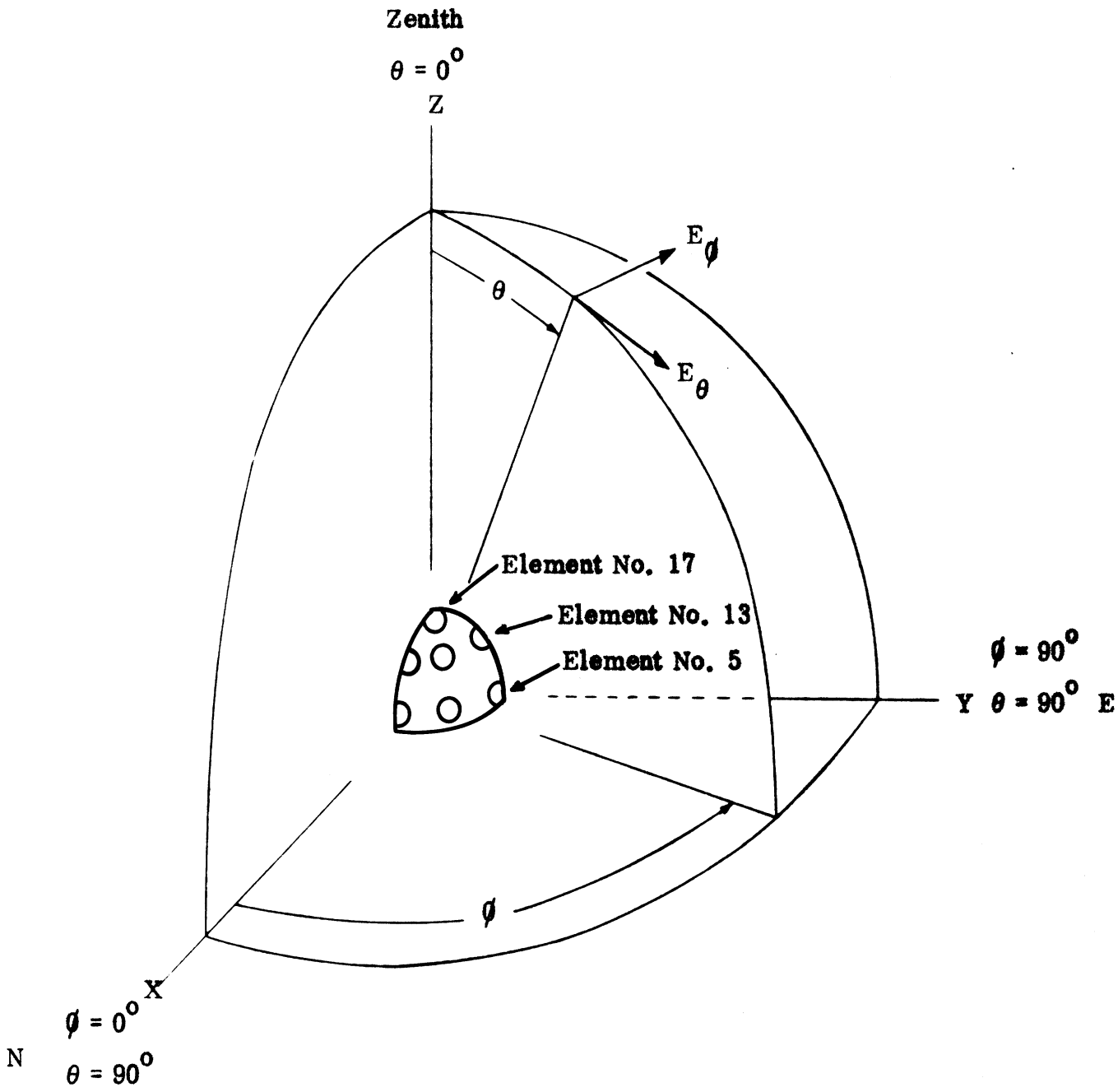

FIG. 4-3: Azimuth - Elevation Coordinate System

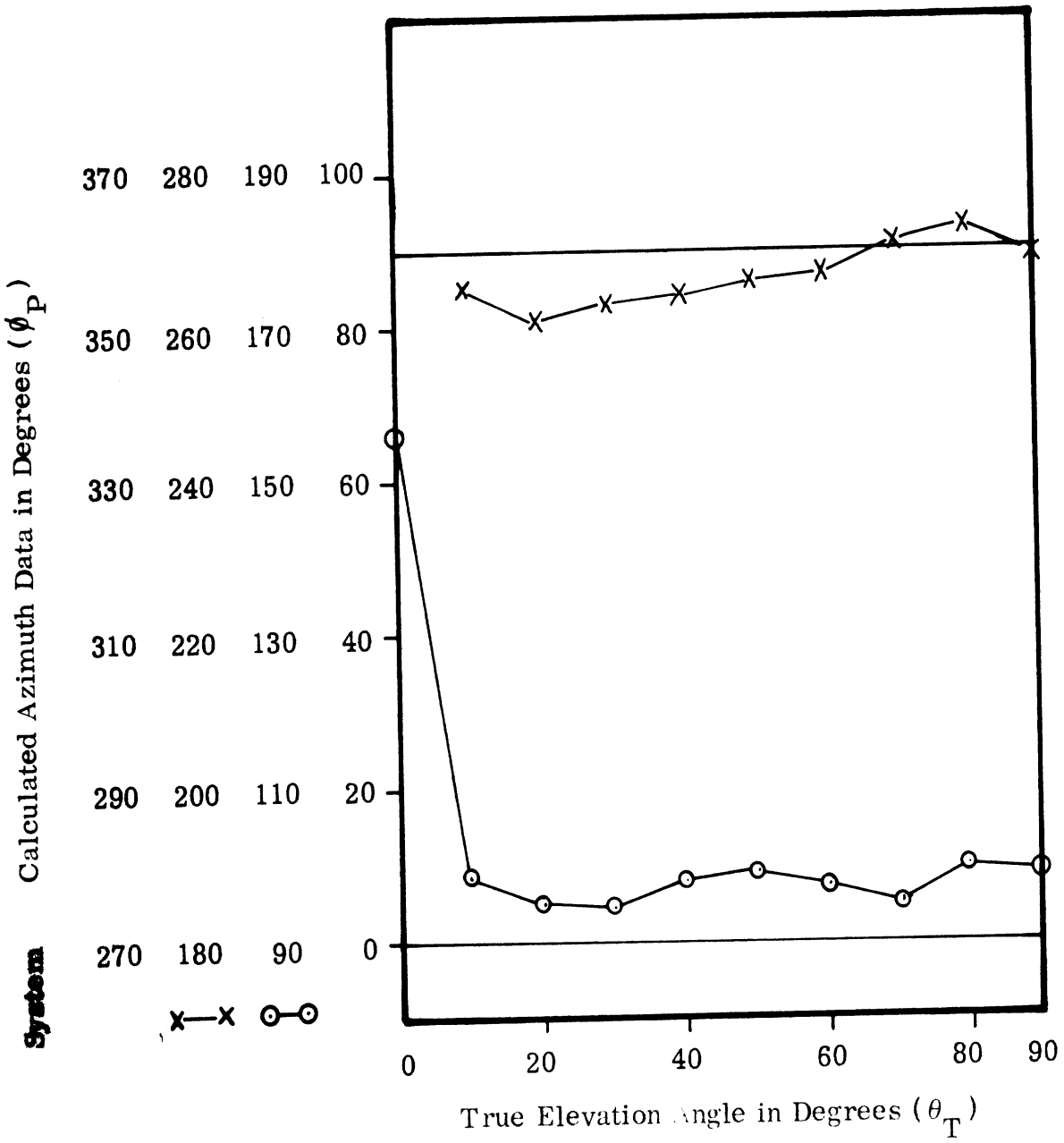

FIG. 4-4: Azimuth Angle as Generated by the DF System as a Function of the True Elevation Angle for $\phi = 90^o$ ⊙—⊙ and $\phi = 270^o$ x—x.

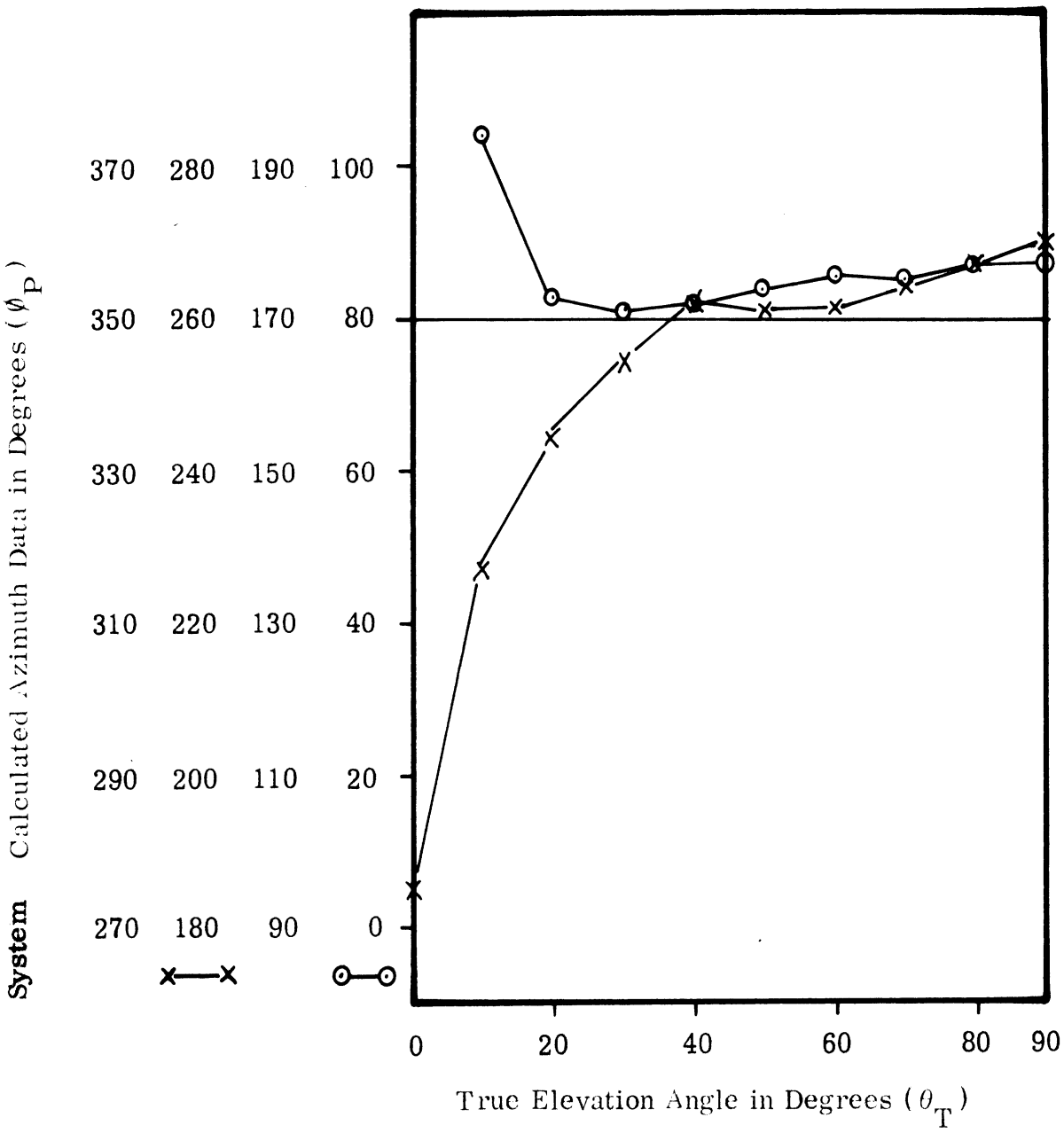

FIG. 4-5: Azimuth Angle as Generated by the DF System as a Function of the True Elevation Angle for $\phi = 80^{o}$ ⊙—⊙ and $\phi = 260^{o}$ ×—× .

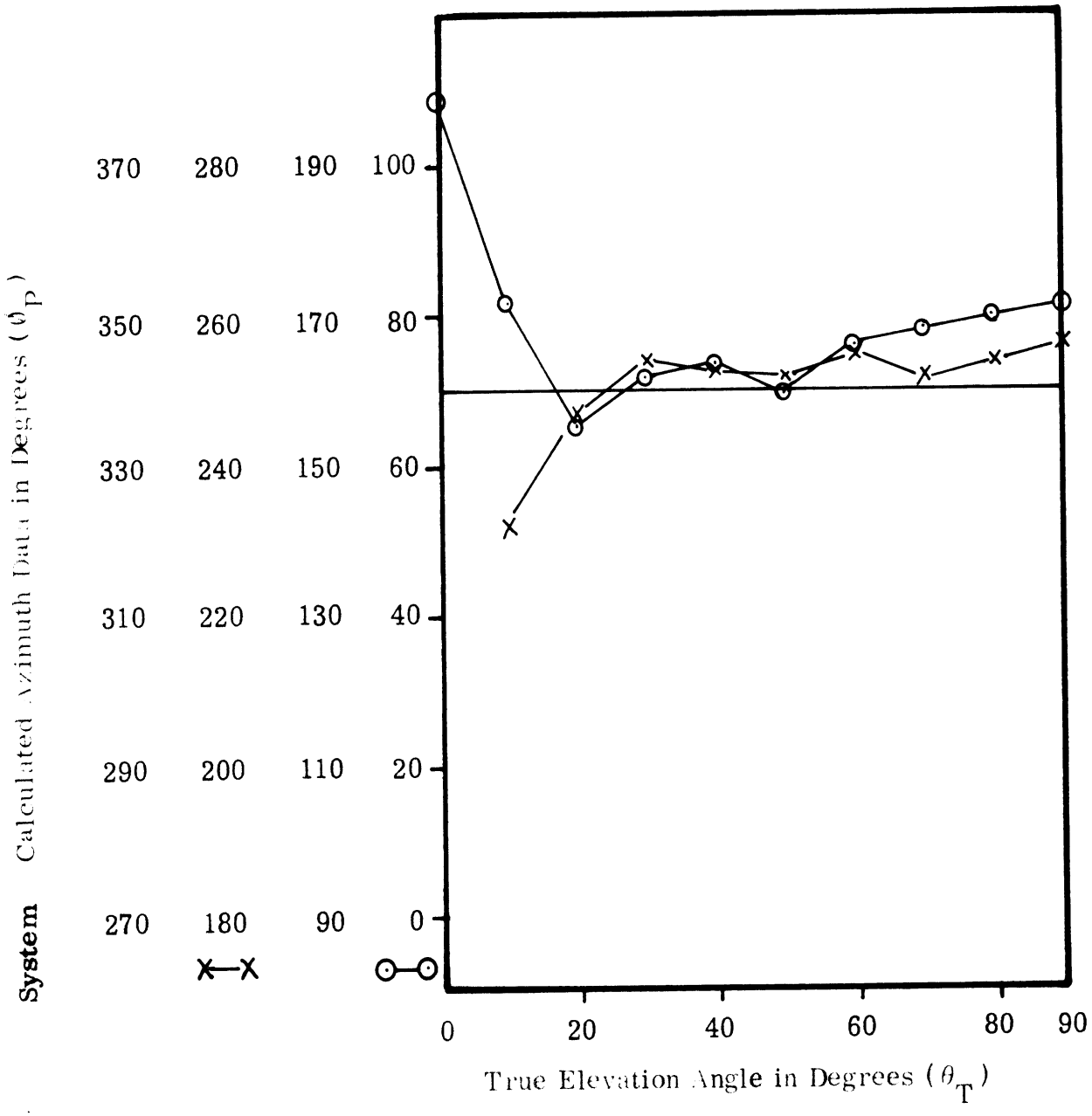

FIG. 4-6: Azimuth Angle as Generated by the DF System as a Function of the True Elevation Angle for $\phi = 70^{\circ}$ O—O and $\phi = 250^{\circ}$ X—X.

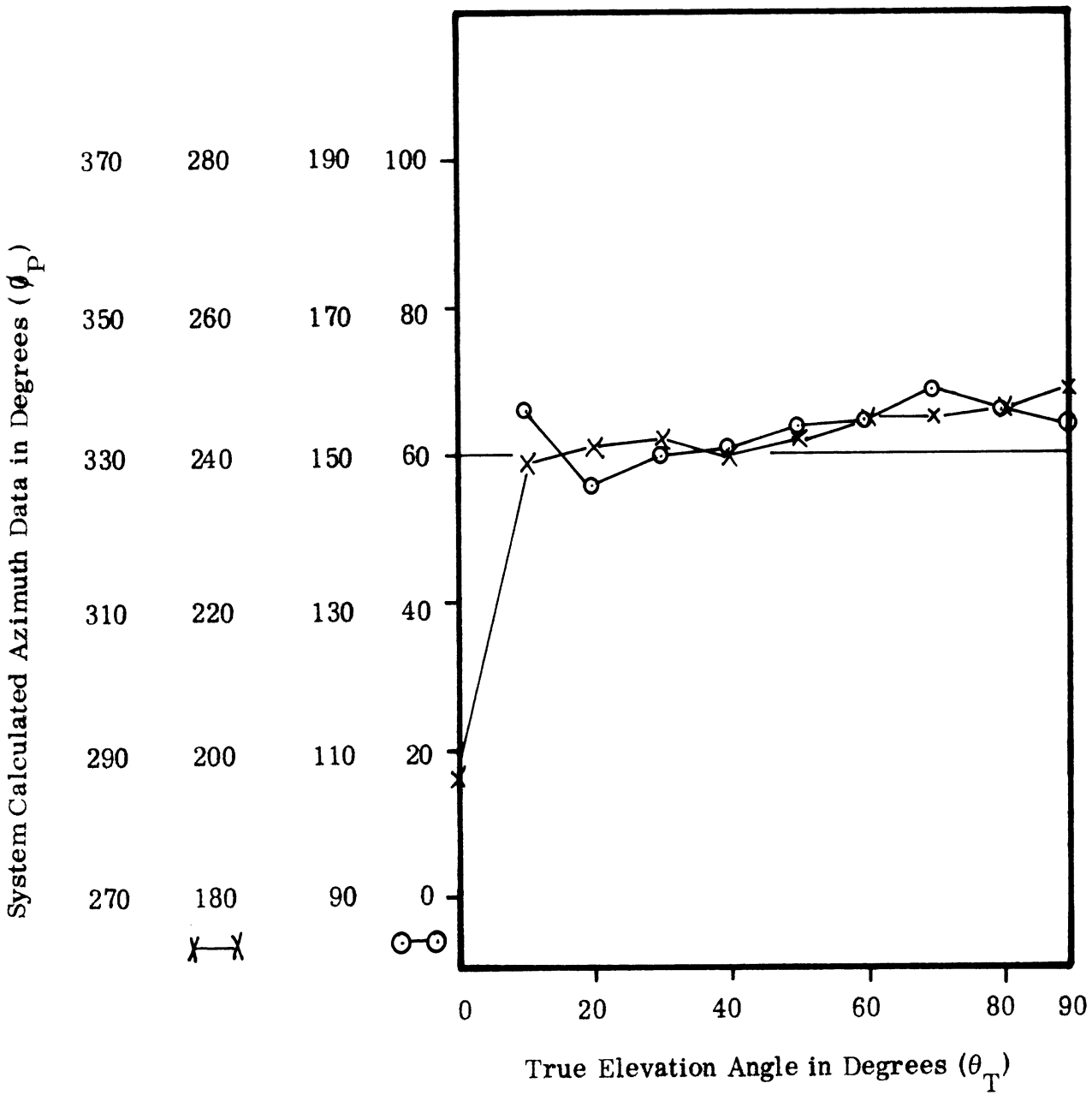

FIG. 4-7: Azimuth Angle as Generated by the DF System as a Function of the True Elevation Angle for $\phi = 60^{\circ}$ ⊙—⊙ and $\phi = 240^{\circ}$ X—X.

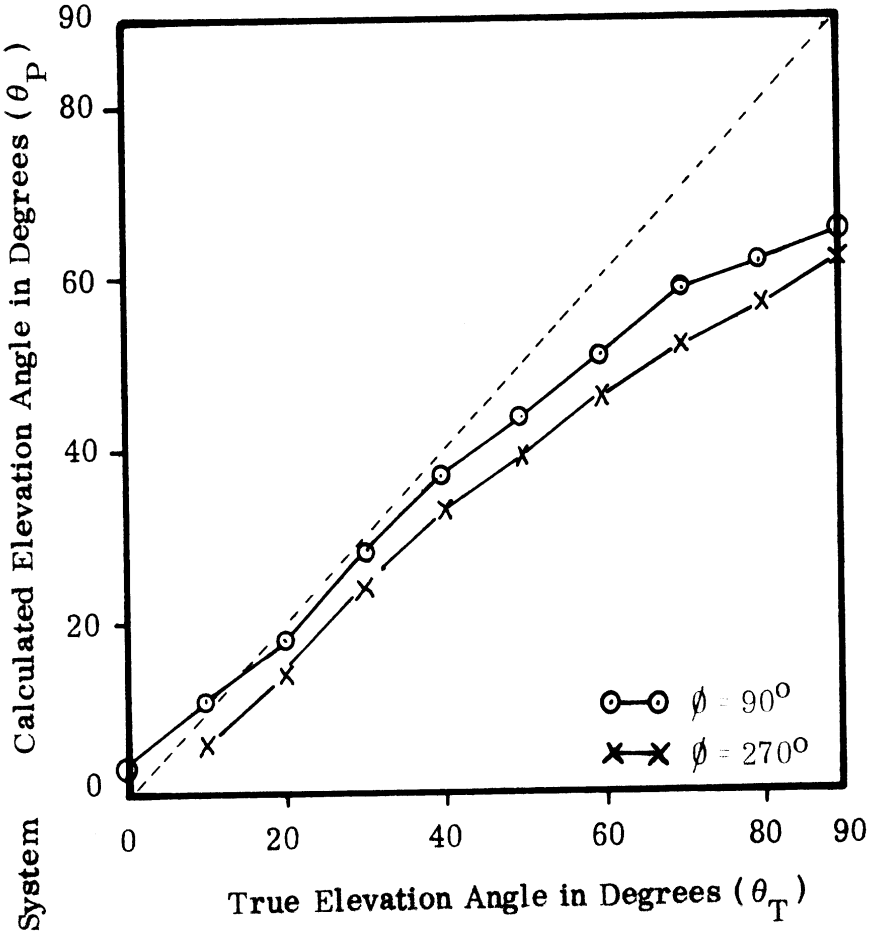

FIG. 4-8: System Generated Elevation Angle vs. True Elevation Angle (Frequency = 1.6 GHz).

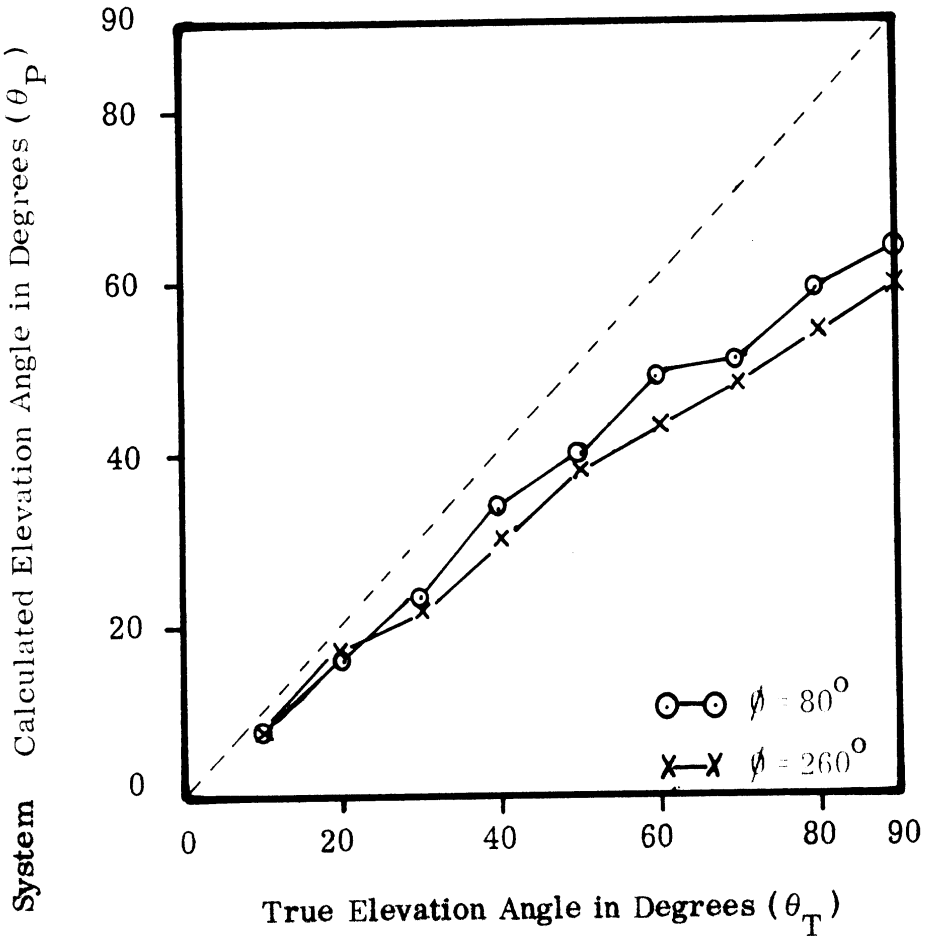

FIG. 4-9: System Generated Elevation Angle vs. True Elevation Angle (Frequency = 1.6 GHz).

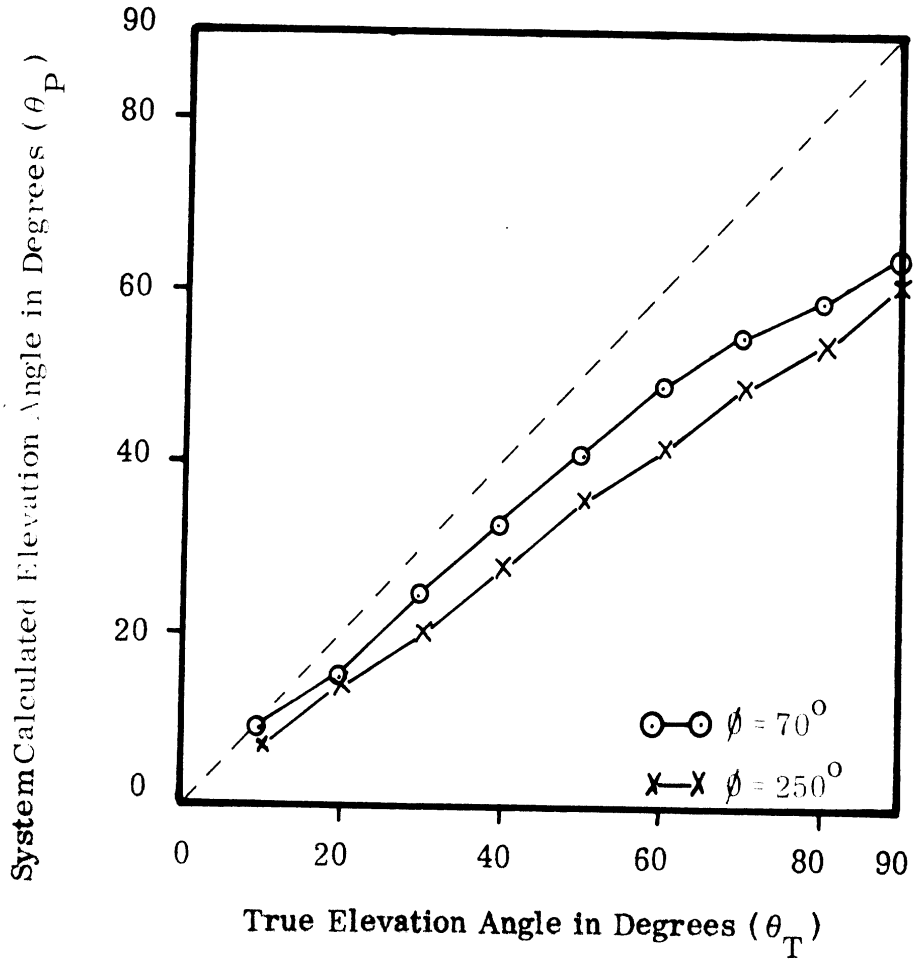

FIG. 4-10: System Generated Elevation Angle vs. True Elevation Angle (Frequency = 1.6 GHz).

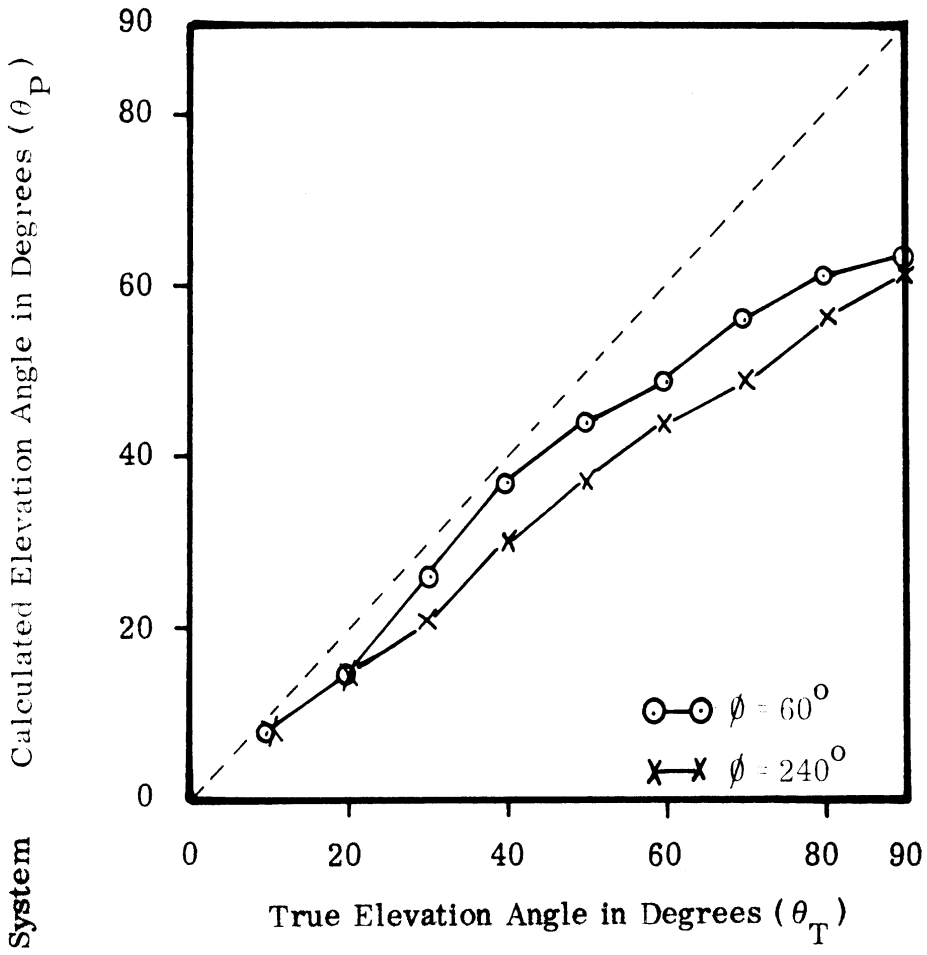

FIG. 4-11: System Generated Elevation Angle vs True Elevation Angle (Frequency = 1.6 GHz).

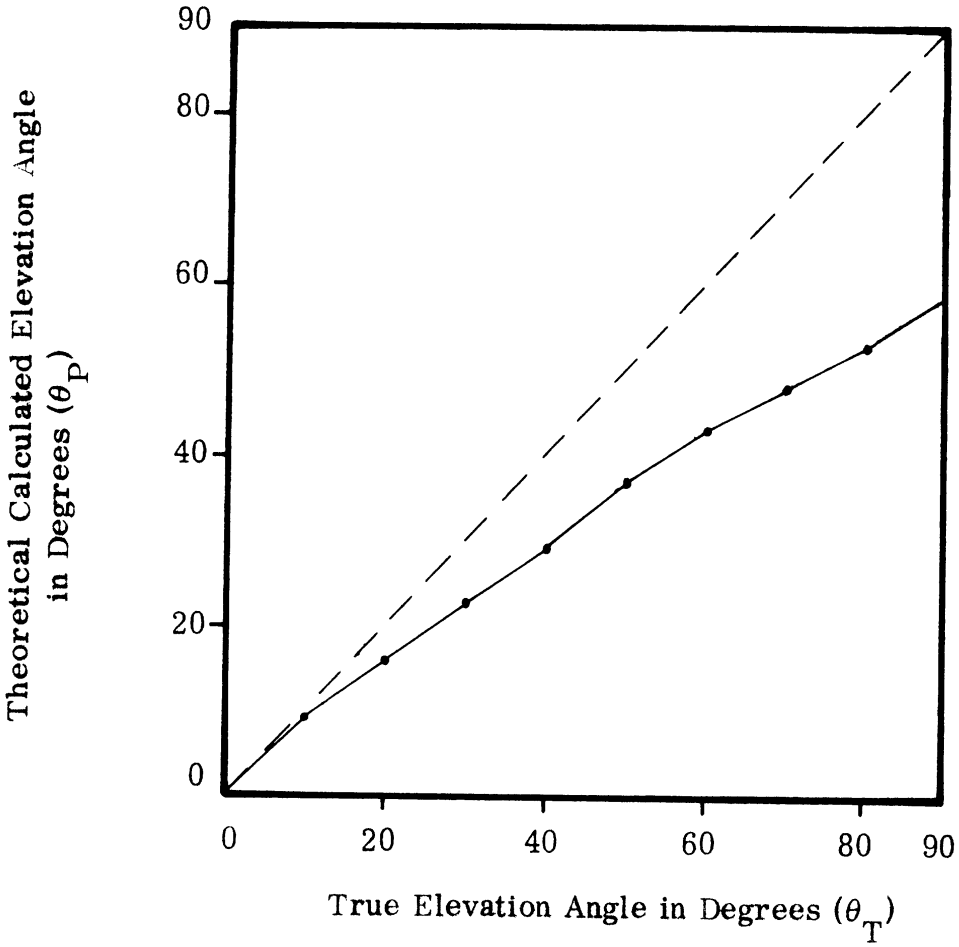

FIG. 4-12: Theoretical Calculated Elevation Angle vs. True Elevation Angle (Assuming a Cosine Element Pattern With Elements Placed at $\theta = 40^{\circ}$ and 80°).

The system response as a function of frequency is graphed in Figs. 4-13 through 4-16. Figures 4-13 and 4-14 are azimuth and elevation data collected at 1.4 GHz with an azimuth angle of $\phi=60^{o}$. Figures 4-15 and 4-16 show the variations of the calculated azimuth and elevation angles as a function of frequency. Note that this data was collected at a fixed azimuth and elevation angle.

The data presented above has been collected employing a CW source. In addition, some tests have been made employing pulsed signals. The pulse data employed a pulse width of approximately 4 microseconds duration and a repetition rate of 1000 pulses per second. This data agreed well with the CW data presented above.

The results of the experiments described above suggest that the A-EDF system has a pointing accuracy of at least $\pm 5^{o}$ in both elevation and azimuth at an operating frequency of 1.6 GHz.

The system response with respect to frequency is not constant. Errors as large as 30^{o} have been measured in azimuth at some frequencies. For this reason most of the preliminary investigation was limited to a single frequency. Since these tests were run, the computer program has been modified to include the elevation correction factor as shown in Fig. 4-12. Subsequent tests were performed to insure that the correction factor functioned properly. However, these tests were not documented and no data is available for presentation. Other program modifications include an averaging subroutine to reduce the effects of random variations in the data, and a subroutine which limits the amount of data used by the computer to make a direction decision. These modifications are discussed in more detail in the System Operation Manual (Section 3.1.2 "Variable Instructions) which was prepared under Contract DAAB07-67-C-0547.

4.2 Fly-By Tests

The fly-by series of tests were designed to evaluate the effect of ground reflections on the A-EDF system performance under dynamic environmental conditions. To conduct these tests the A-EDF system was installed at The University of Michigan's NIKE-Ajax radar site. A photograph of the radar site and sketch of the A-EDF system installation appears in Figs. 4-17 and 4-18 respectively.

A 1.6 KHz CW source was installed in a DC-3 aircraft and the aircraft tracked simultaneously by the A-EDF system and the NIKE-Ajax radar. The aircraft maneuvered in a random fashion around the vicinity of the test site at an altitude of approximately 10,000 feet and ranges from two to ten miles. The NIKE-Ajax radar coordinates were correlated with the A-EDF system by the use of a data multiplex switch which read the radar coordinates into the A-EDF system computer. This data was then printed out on the A-EDF system teletype. The data multiplex switch and voltage scaling networks are described in the Appendix of the Final Report prepared under this contract (ECOM-6-0547, 1084-6-F).

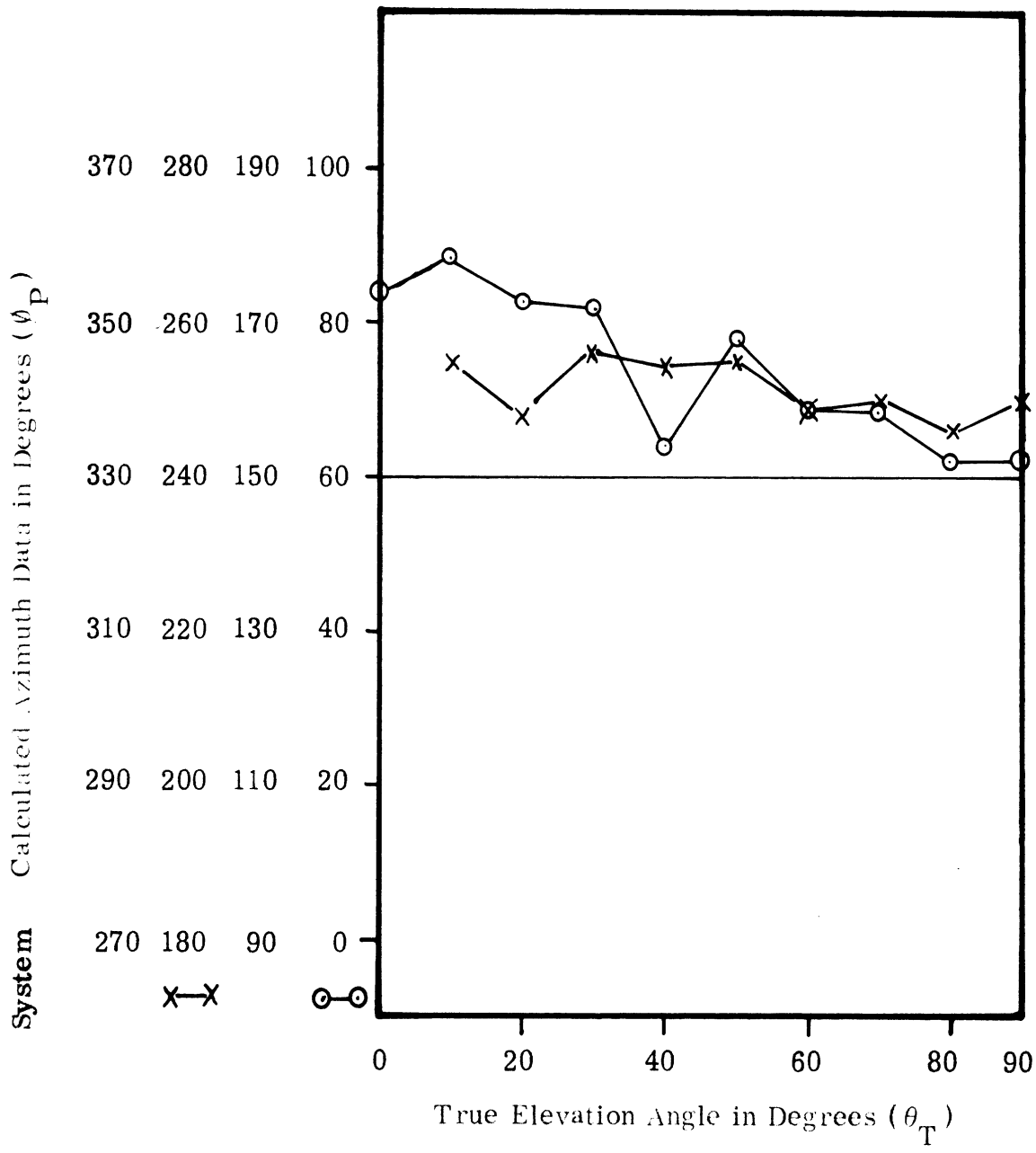

FIG. 4-13: System Generated Azimuth Angle vs. True Elevation Angle (Frequency 1.4 GHz) for ϕ 60° ⊙—⊙ and 240° X—X .

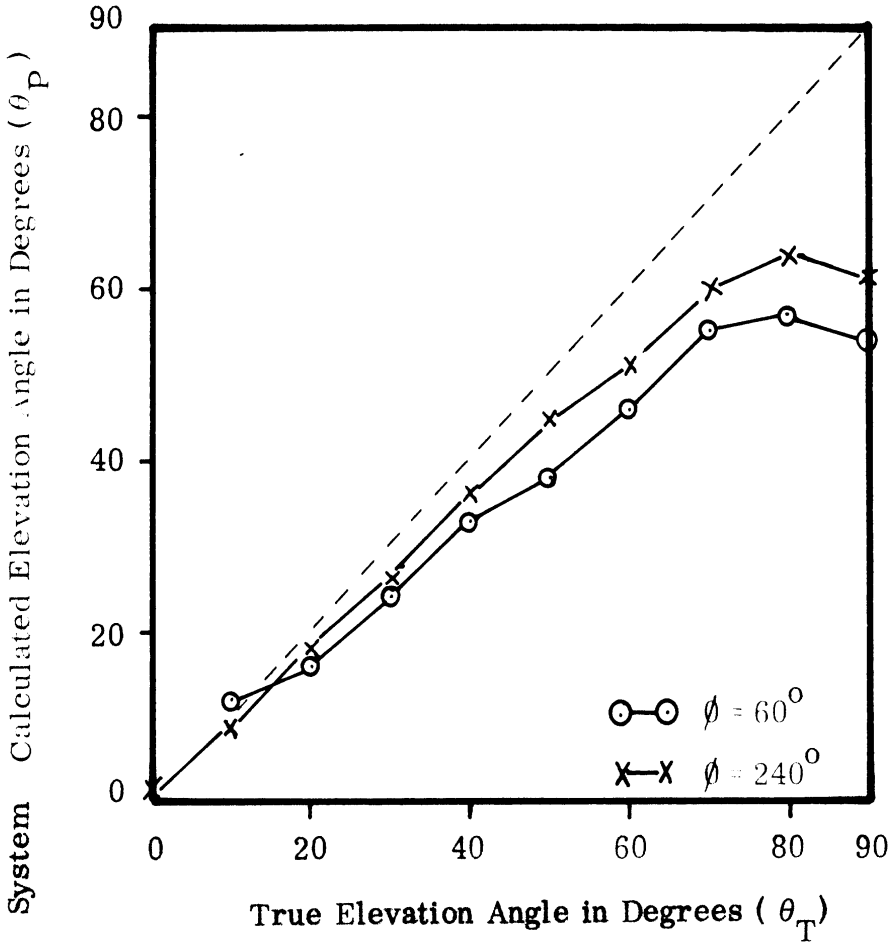

FIG. 4-14: System Generated Elevation Angle vs. True Elevation Angle (Frequency = 1.4 GHz).

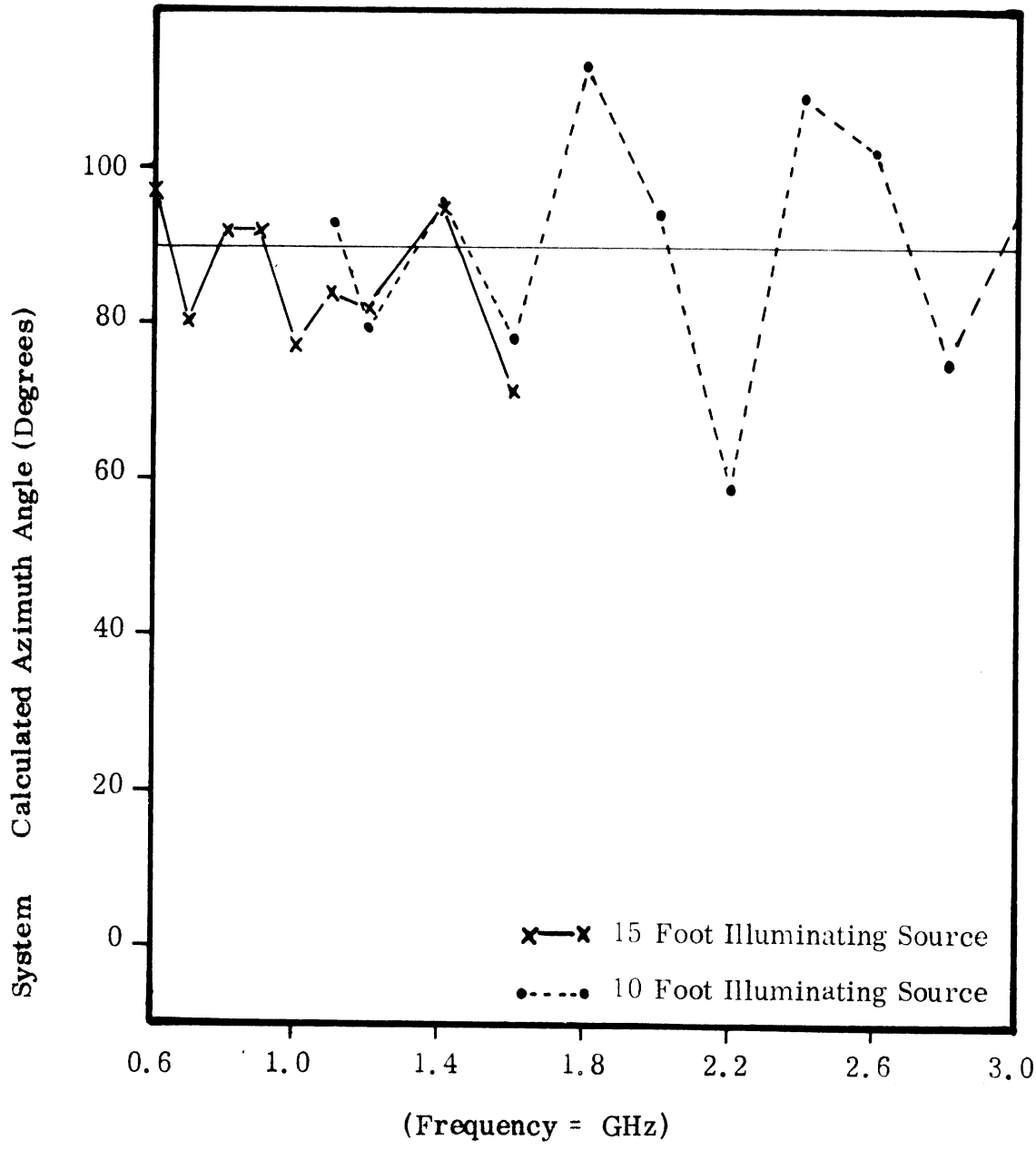

FIG. 4-15: System Generated Azimuth Angle vs. Frequency for a Fixed Azimuth and Elevation of Illuminating Source ($\theta = 90^{o}$, $\phi = 30^{o}$).

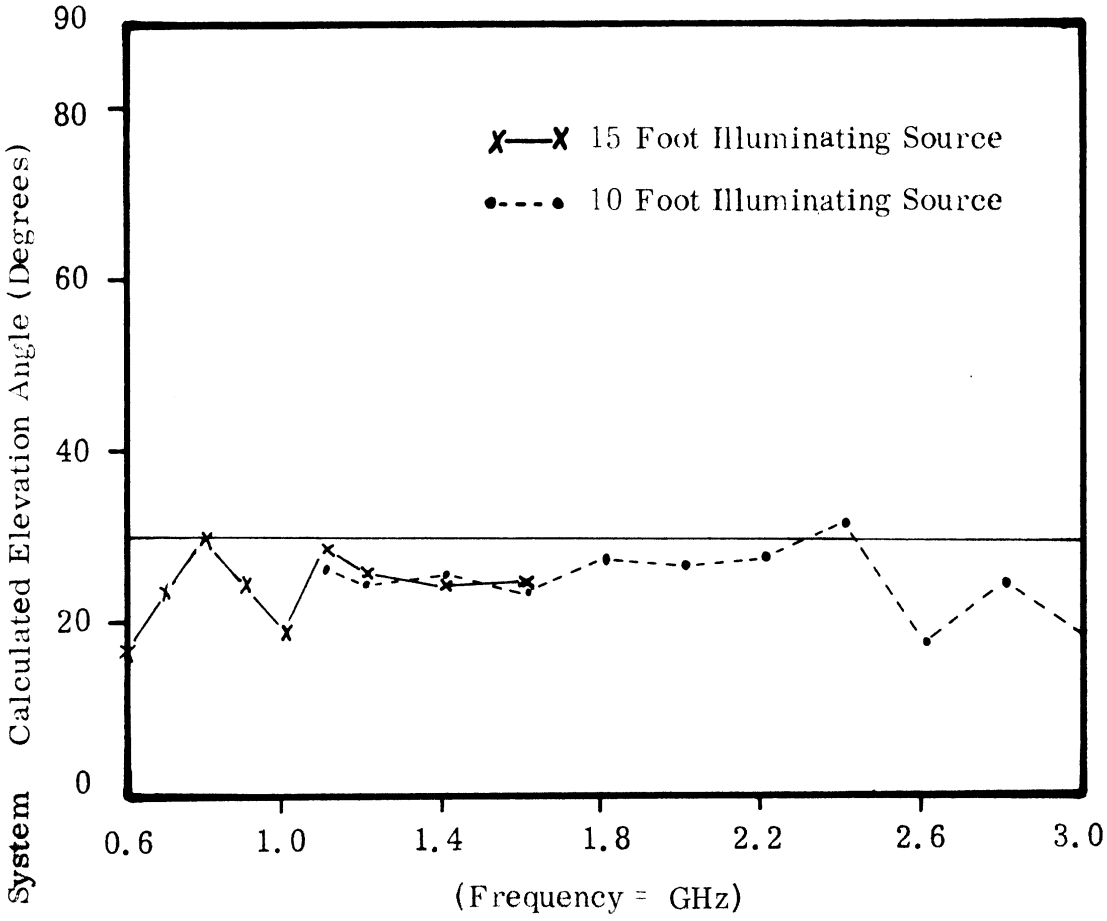

FIG. 4-16: System Generated Elevation Angle vs. Frequency for a Fixed Azimuth and Elevation of Illuminating Source ($\theta = 90^{o}$, $\phi = 30^{o}$).

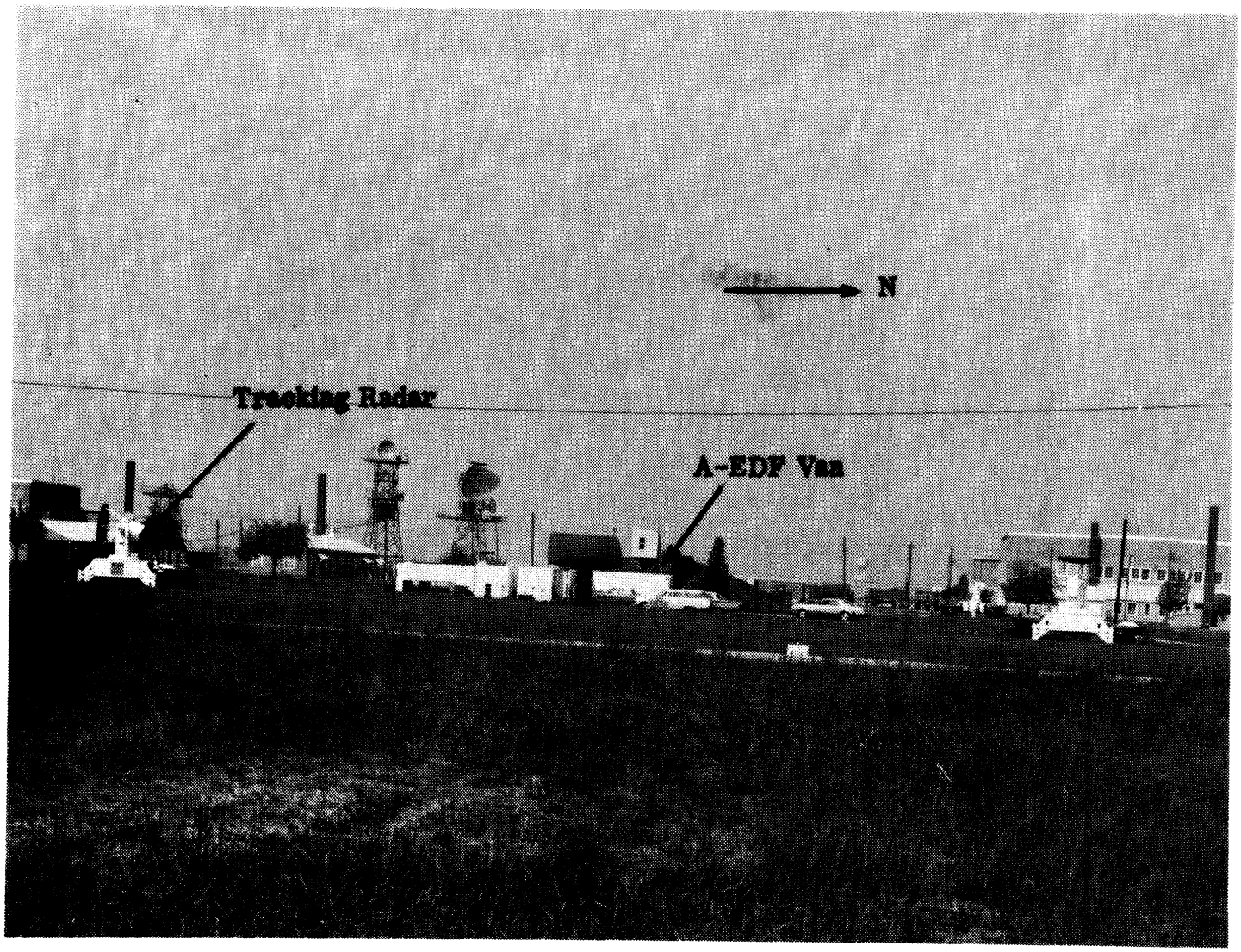

FIG. 4-17: Photograph of Test Site for Fly-By Tests.

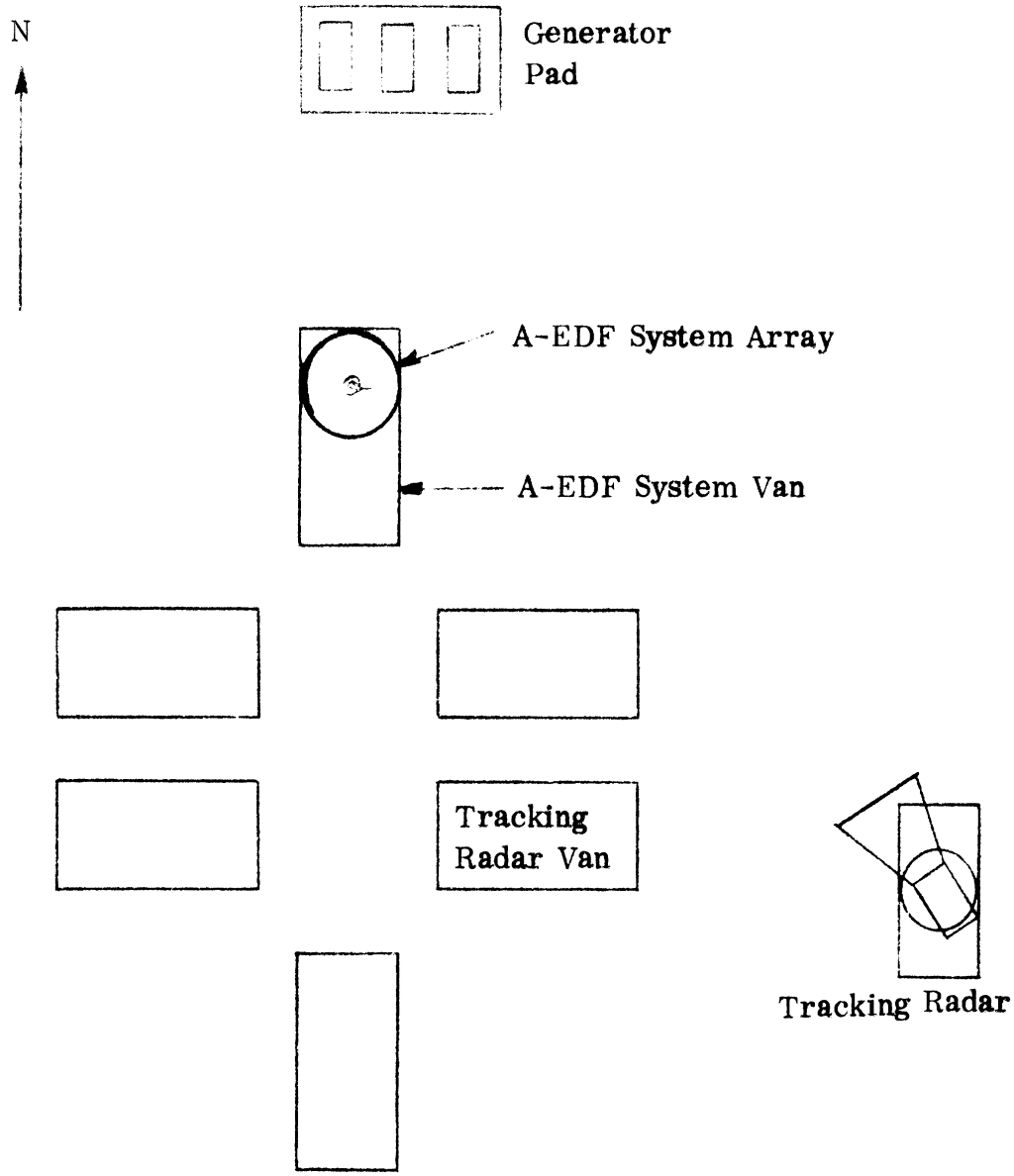

FIG. 4-18: Sketch of A-EDF System/Nike Radar Site During Fly-By Tests (not to scale).

The results of the fly-by tests appear in Table 4.1 . For the 60 data samples collected, the average azimuth error and standard deviations were 1.55° and 5.9° respectively. If the error distribution were normal (Gaussian) the average error would be zero. Assuming the distribution is normal, one would expect the error on 68 percent of the data points to lie within the standard deviation. Of the data collected, 77 percent of the points were within ± 6°, suggesting that the assumption of a Gaussian distribution is acceptable and conservative. The average elevation error and standard deviations were 0.53° and 7.5° respectively. Seventy-two percent of the elevation data points collected had an error of less than or equal to 8°. The error distribution is slightly skewed from the normal, but conforms well to the results predicted by assuming a normal distribution. It should also be noted that the radar data presented in Table 4.1 has associated with it a random uncertainty of ± 1° due to the processing of the data through the multiplexer and scaling amplifier.

Referring to Figs. 4-17 and 4-18 one can easily see that the possibility of multiple signal paths is high. An example is diagrammed in Fig. 4-19. Due to the irregular nature of the positions and geometries of the reflecting objects and the irregular flight paths of the aircraft, little correlation exists between a specific azimuth or elevation angle and the error experienced at that angle. It is highly improbable that the contribution of the reflections to the A-EDF system output can be quantitatively evaluated from these tests.

A second known source of uncertainty is the low signal-to-noise ratio of the signals received during these tests. Knowing the output power of the airborne source, the transmitting and receiving antenna gains and the signal path attenuation, one can calculate the magnitude of the received signal. With the aid of the path length versus attenuation graph in Fig. 4-20, the computations indicated above are performed in Table 4.2. The results of the computations, which are graphed in Fig. 4-21, indicate that for a range of two miles, the signal power into the receiver is a maximum of -62 to -72 dBm . Previous experience with the A-EDF system has indicated that a minimum signal power of -70 dBm into the receiver (Micro-Tel WR-200) is necessary for a 6 dB signal-to-noise ratio into the peak reading voltmeter which is the very minimum signal-to-noise ratio for meaningful system operation. An input signal of -55 dBm is the minimum desirable input level. The signals received during these tests were seldom more than the absolute minimum required for system operation, and could at times be observed receding into the noise. It should also be noted that the signal levels in Fig. 4-21 are somewhat optimistic since the airborne antenna was a monopole, vertically polarized with respect to the wings of the aircraft and exhibited somewhat less than 0 dB gain at elevation angles near the zenith. As a result of these tests, the computer program has been modified to reject data below a minimum signal-to-noise ratio selected by the operator.

TABLE 4-1a

Results of Fly-By Tests

	Azimuth (degrees)			Elevation (degrees)		
Sample	A-EDF System	Radar	Δ^{o}_{A}	A-EDF System	Radar	Δ^{o}_{E}
1	204	208	-4	51	65	-14
2	269	267	+2	21	31	-10
3	172	173	-1	69	61	+8
4	32	40	-6	30	21	+9
5	173	172	+1	54	61	-7
6	289	287	+2	40	44	-4
7	164	159	+5	40	29	+11
8	195	195	0	57	64	-7
9	274	282	-8	46	61	-15
10	307	316	-9	36	37	-1
11	198	201	-3	59	58	+1
12	329	319	+10	31	30	+1
13	331	325	+6	42	38	+4
14	16	10	+6	42	30	+12
15	12	8	+4	42	27	+15
16	18	23	-5	15	17	-2
17	50	46	+4	22	11	+11
18	276	278	-2	25	24	+1
19	285	284	+1	18	23	-5
20	353	347	+6	28	30	-2
21	16	7	+9	40	29	+11
22	14	7	+7	33	34	-1
23	218	228	-10	33	31	+2
24	318	329	-11	40	38	+2
25	338	331	+7	49	50	-1
26	325	329	-2	40	49	-9
27	352	349	+3	52	65	-13
28	352	351	+1	57	63	-6
29	41	35	+6	54	66	-8
30	43	38	+5	62	66	-4

TABLE 4-1a (continued)

Sample	A-EDF System	Radar	Δ^{o}_{A}	A-EDF System	Radar	Δ^{o}_{E}
31	58	60	-2	55	56	-1
32	71	65	+6	54	58	+4
33	75	72	+3	62	58	+4
34	106	107	-1	62	58	+4
35	144	144	0	64	68	-4
36	198	188	+10	55	54	+1
37	266	266	0	21	26	-5
38	344	335	+9	15	19	-4
39	67	68	-1	1	2	-1
40	151	141	+10	7	8	-1
41	200	191	+9	31	33	-2
42	5	16	-11	34	24	+10
43	84	77	+7	51	36	+15
44	154	154	0	43	44	-1
45	14	17	-3	39	24	+15
46	25	22	+3	43	30	+13
47	15	10	+5	45	49	-4
48	14	23	-9	37	30	+7
49	322	317	+5	18	10	+8
50	317	310	+7	19	23	-4
51	325	315	+10	31	31	0
52	333	325	+8	36	37	-1
53	331	327	+4	36	40	-4
54	325	331	-6	40	43	-3
55	7	11	-4	52	61	-9
56	35	31	+4	31	17	+15
57	176	175	+1	60	59	+1
58	183	181	+2	69	63	+6
59	194	197	-3	66	71	-5
60	196	197	-1	71	72	-1

TABLE 4-1 (b)

Summary of Statistical Results

Average Azimuth Error

$$\bar{\Delta}_A = \frac{\sum_{n=1}^{N} \Delta A_n}{N} = +1.55^o$$

Azimuth Standard Deviation

$$\sigma_A = \sqrt{\frac{\sum_{n=1}^{N} \Delta A_n^2}{N-1}} = 5.9^o$$

Average Elevation Error

$$\bar{\Delta}_E = \frac{\sum_{n=1}^{N} \Delta E_n}{N} = +.53^o$$

Elevation Standard Deviation

$$\sigma_E = \sqrt{\frac{\sum_{n=1}^{N} \Delta E_n^2}{N-1}} = 7.5^o$$

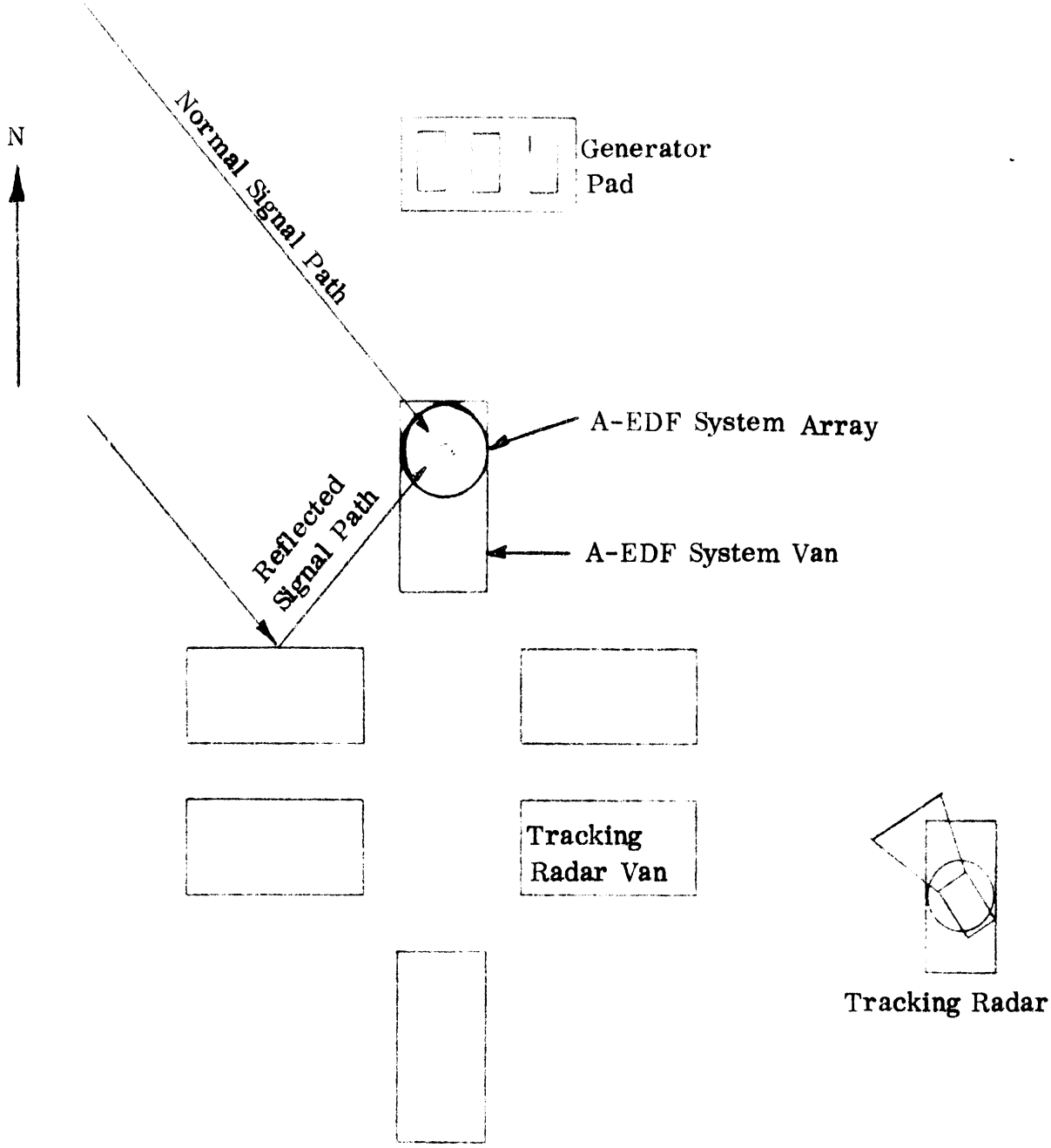

FIG. 4-19: Example of Multiple Path Reflection

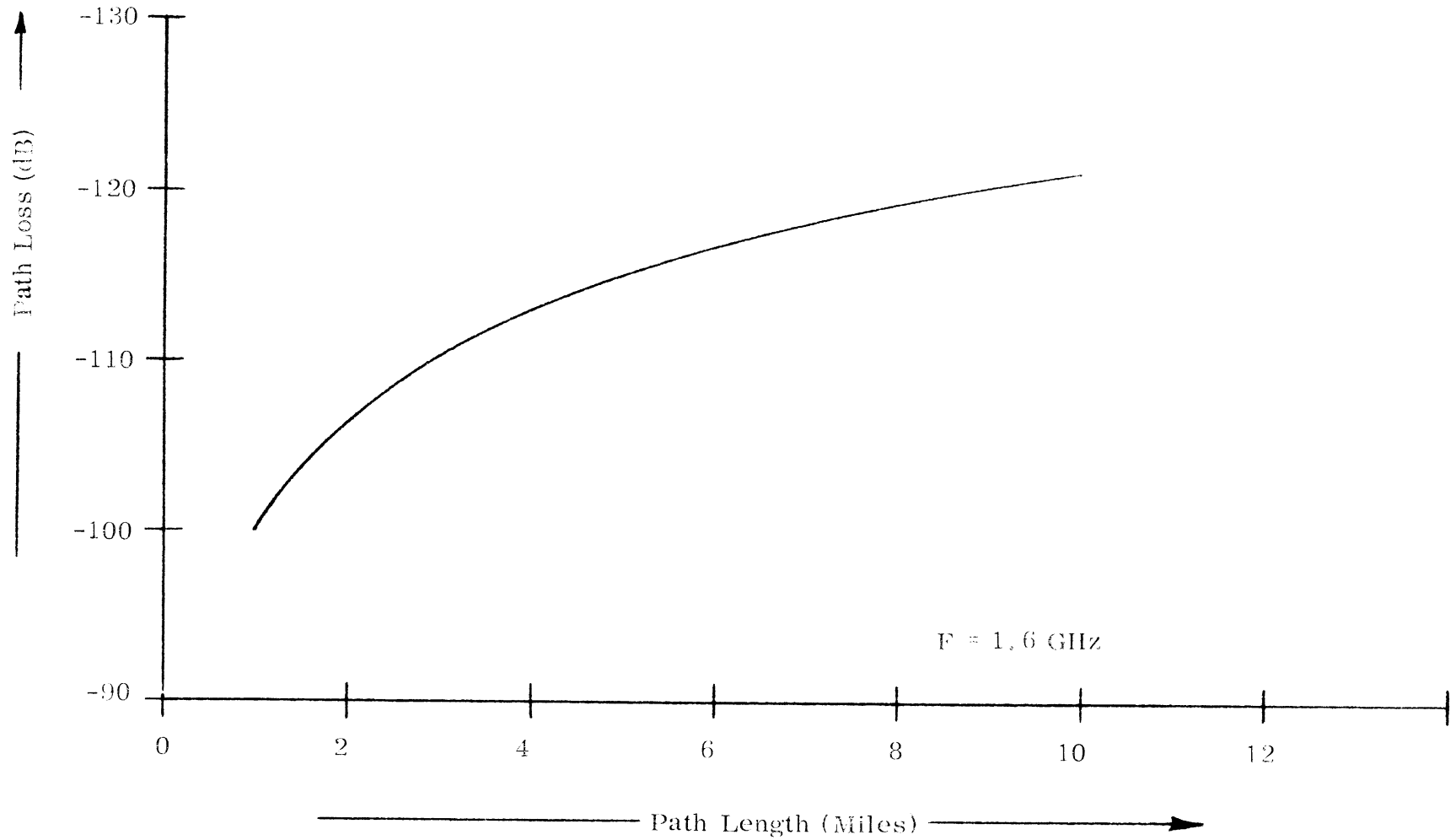

FIG. 4-20: Path Loss versus Path Length.

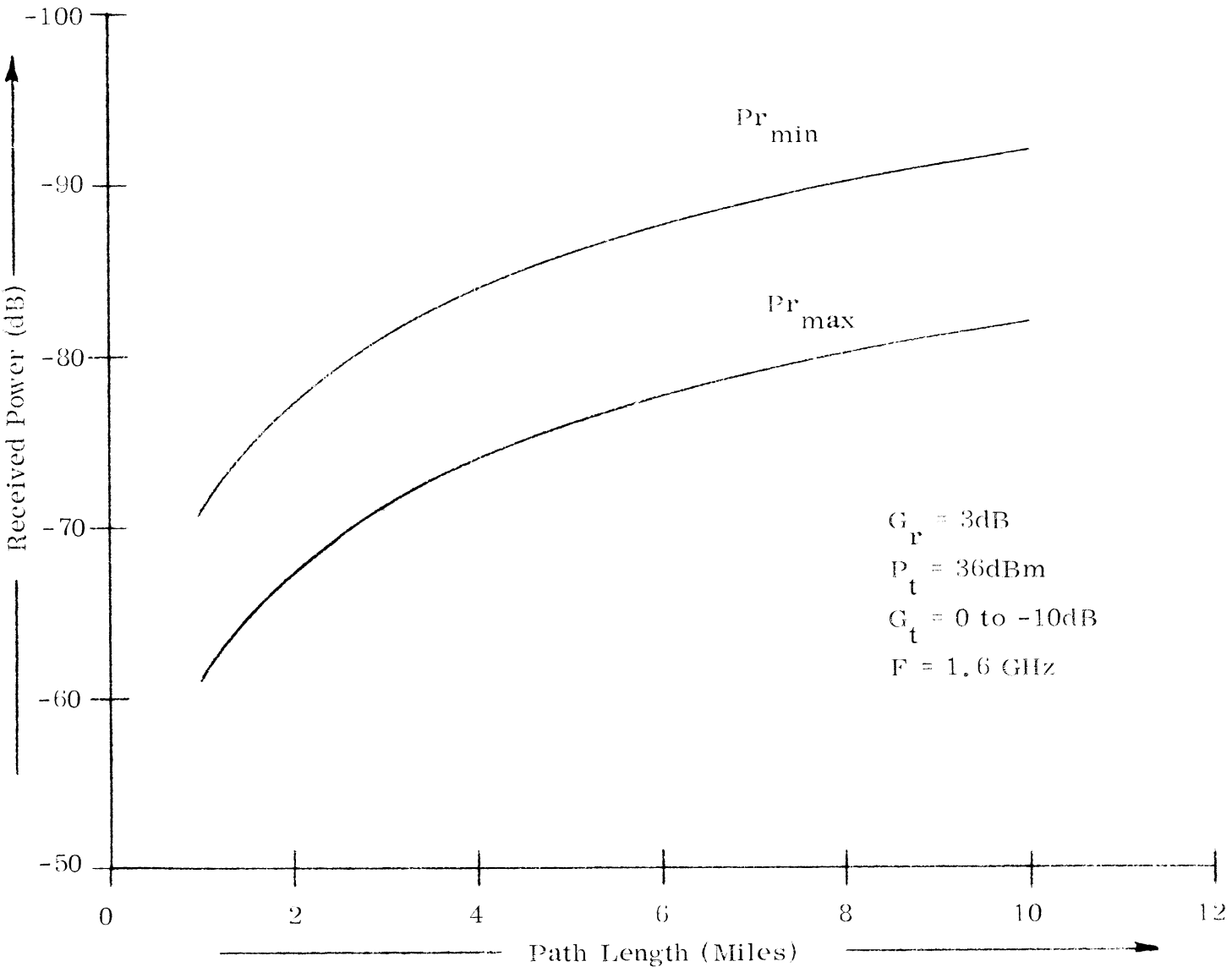

FIG. 4-21: Received Power versus Path Length.

TABLE 4.2

Computations for Received Power

$$P_r = P_t + G_t + G_r + N_r$$

where

P_r = Received Power (dBm)

P_t = Transmitted Power (dBm) = +36dBm (4 watts)

N_r = Path Loss (dB)

G_r = Receiving Antenna Gain (dB) = +3dB Above a Linearly Polarized Isotrope

G_t = Transmitting Antenna Gain (dB) = +0 to -10dB above a Linearly Polarized Isotrope

such that

$$P_r = 39\text{dBm} + N_r$$

5.0 CONCLUSIONS AND RECOMMENDATIONS

From the results presented in this report, it has been concluded that the A-EDF system approaches the bearing accuracy performance goal at discrete frequencies (i.e. 1.6 GHz) under free space conditions, but is adversely affected by frequency variations and a severe electrical environment. The free space bearing accuracy at 1.6 GHz is approximately $\pm 5^{o}$ in both azimuth and elevation. However , there is nothing inherent in this technique for azimuth-elevation direction finding which limits the bearing accuracy to $\pm 5^{o}$. A quantitative evaluation of the system accuracy and accuracy degradation due to imperfect component performance is given in the Final Report under this contract (Chapter III, System Error Analysis). The system bearing accuracy during the fly-by tests was about $\pm 6^{o}$ in azimuth and $\pm 8^{o}$ in elevation. It is felt that the performance degradation from the free space condition was due to the hostile environment. Low signal amplitude and the resultant high signal-to-noise ratio of the data and the high probability of multiple path reflections are felt to be major sources of error.

As a result of the A-EDF system tests described in the preceding chapter, the computer program has been modified to include several improvements. These modifications include an averaging method which allows the operator to select the number of data points to be averaged before the display is changed, a command which limits the amount of data used to make a given bearing computation, and a routine that inhibits the display if sufficient signal is not present to provide accurate results. A more detailed description of these modifications can be found in the A-EDF system Operator's Manual prepared under this contract (ECOM-7-0547, 1084-7-OM, Section 3.1.2 "Variable Instructions").

The results of the tests documented above are not to be construed as a complete description of the A-EDF performance. These tests were designed primarily as design aids to compliment the system development. It is recommended that a much more complete testing program be initiated. Such a program might include: 1) a complete series of free space tests utilizing CW modulation at a single frequency where the antennas perform well (e.g. 1.6 GHz), 2) free space tests employing other modulation types, 3) free space tests at other frequencies, and finally, 4) dynamic environmental tests with the system installed at the testing site as recommended in Chapter II of the A-EDF system Operator's Manual.